THE JOURNAL OF BIOLOGICAL CHEMISTRY VOL. 286, NO. 36, pp. 31337–31346, September 9, 2011

Specific Enzyme Complex of β-1,4-Galactosyltransferase-II and Glucuronyltransferase-P Facilitates Biosynthesis of *N*-linked Human Natural Killer-1 (HNK-1) Carbohydrate*[S]

Received for publication, February 21, 2011, and in revised form, July 5, 2011 Published, JBC Papers in Press, July 19, 2011, DOI 10.1074/jbc.M111.233353

Tetsuya Kouno[‡], Yasuhiko Kizuka[§1], Naoki Nakagawa[‡], Toru Yoshihara[¶‖], Masahide Asano[¶], and Shogo Oka[‡2]

From the [‡]Department of Biological Chemistry, Human Health Sciences, Graduate School of Medicine, and [§]Department of Biological Chemistry, Graduate School of Pharmaceutical Sciences, Kyoto University, Kyoto 606-8507 and the [¶]Division of Transgenic Animal Science, Advanced Science Research Center, and [‖]Research Center for Child Mental Development, Kanazawa University, Kanazawa 920 8640, Japan

Human natural killer-1 (HNK-1) carbohydrate is highly expressed in the nervous system and is involved in synaptic plasticity and dendritic spine maturation. This unique carbohydrate, consisting of a sulfated trisaccharide (HSO_3-3GlcAβ1–3Galβ1–4GlcNAc-), is biosynthesized by the successive actions of β-1,4-galactosyltransferase (β4GalT), glucuronyltransferase (GlcAT-P and GlcAT-S), and sulfotransferase (HNK-1ST). A previous study showed that mice lacking β4GalT-II, one of seven β4GalTs, exhibited a dramatic loss of HNK-1 expression in the brain, although β4GalT-I-deficient mice did not. Here, we investigated the underlying molecular mechanism of the regulation of HNK-1 expression. First, focusing on a major HNK-1 carrier, neural cell adhesion molecule, we found that reduced expression of an *N*-linked HNK-1 carbohydrate caused by a deficiency of β4GalT-II is not likely due to a general loss of the β1,4-galactose residue as an acceptor for GlcAT-P. Instead, we demonstrated by co-immunoprecipitation and endoplasmic reticulum-retention analyses using Neuro2a (N2a) cells that β4GalT-II physically and specifically associates with GlcAT-P. In addition, we revealed by pull-down assay that Golgi luminal domains of β4GalT-II and GlcAT-P are sufficient for the complex to form. With an *in vitro* assay system, we produced the evidence that the kinetic efficiency k_{cat}/K_m of GlcAT-P in the presence of β4GalT-II was increased about 2.5-fold compared with that in the absence of β4GalT-II. Finally, we showed that co-expression of β4GalT-II and GlcAT-P increased HNK-1 expression on various glycoproteins in N2a cells, including neural cell adhesion molecule. These results indicate that the specific enzyme complex of β4GalT-II with GlcAT-P plays an important role in the biosynthesis of HNK-1 carbohydrate.

Glycosylation is a major post-translational modification, especially for cell surface and extracellular proteins, and plays important roles in cellular functions such as adhesion, endocytosis, and receptor signaling (1, 2). In general, glycan is biosynthesized in a stepwise manner by ER[3]- or Golgi-resident glycosyltransferases. As most of these glycosyltransferases have been cloned, there is an overall understanding of the pathway of production. However, the expression of a given glycosyltransferase does not always reflect that of its product, because it has become clear that activities of glycosyltransferases are regulated by oligomerization or proteolytic cleavage (3, 4). In addition, some glycosyltransferases form heterocomplexes that alter their activities, substrate specificity, or distribution in the ER or Golgi apparatus (5, 6). Thus, to understand the functions and biosynthesis of glycans, it is necessary to clarify how the activity of individual glycosyltransferases is regulated in cells.

Human natural killer-1 (HNK-1) carbohydrate is highly expressed on several cell adhesion molecules in the nervous system, including the neural cell adhesion molecule (NCAM) (7, 8). HNK-1 carbohydrate has a unique structure, including a sulfated trisaccharide (HSO_3-3GlcAβ1–3Galβ1–4GlcNAc-) (9, 10), and is biosynthesized by the successive actions of β-1,4-galactosyltransferase (β4GalT), a glucuronyltransferase (GlcAT-P or GlcAT-S), and a sulfotransferase (HNK-1ST) (11–13). We previously generated mice lacking the gene for GlcAT-P, a major glucuronyltransferase in the nervous system (14). The GlcAT-P-deficient mice showed an almost complete loss of HNK-1 expression in the brain and exhibited reduced long term potentiation at hippocampal CA1 synapses along with impaired maturation of dendritic spines, indicating an important role for this glycan in synaptic plasticity (14, 15). In terms of the expression, we have been uncovering well controlled mechanisms of HNK-1 biosynthesis. For instance, GlcAT-P (S) and HNK-1ST form a functional complex, and the distribution of GlcAT-P in the Golgi is regulated by a small GTPase (16). However, it is still unclear how the inner *N*-acetyllactosamine structure (Galβ1–4GlcNAc) for HNK-1 carbohydrate is synthesized and how HNK-1 is selectively attached to limited kinds of carrier proteins.

* This work was supported in part by Grant-in-aid for Scientific Research (B) 21370053 (to S. O.) from the Ministry of Education, Culture, Sports, Science and Technology and in part by the Ministry of Health, Labor, and Welfare of Japan Health and Labour Sciences Research Grant on Comprehensive Research on Disability Health and Welfare, H21-012.

[S] The on-line version of this article (available at http://www.jbc.org) contains supplemental Figs. 1–3.

[1] Present address: Disease Glycomics Team, Systems Glycobiology Research Group, Advanced Science Institute, RIKEN, Saitama 351-0198, Japan.

[2] To whom correspondence should be addressed: Kawahara-cho 53, Shogoin, Sakyo-ku, Kyoto 606-8507, Japan. Tel./Fax: 81-75-751-3959; E-mail: shogo@hs.med.kyoto-u.ac.jp.

[3] The abbreviations used are: ER, endoplasmic reticulum; β4GalT, β1,4-galactosyltransferase; GlcAT, glucuronyltransferase; HNK-1, human natural killer-1; PSA, polysialic acid; PST, polysialyltransferase; NCAM, neural cell adhesion molecule; ASOR, asialo-orosomucoid.

Although the β4GalT family is known to have seven members (β4GalT-I to VII) *in vivo* (17, 18), the biological role of each is not fully understood. Some of them are able to synthesize *N*-acetyllactosamine on glycoproteins. which is potentially further modified by GlcAT-P. We recently reported that β4GalT-II-deficient mice showed similar phenotypes to GlcAT-P-deficient mice with a reduction in HNK-1 expression and impaired spatial learning and memory (19), although HNK-1 expression was unaltered in the β4GalT-I-deficient mouse brain (20) despite the similarity in primary structure and acceptor specificity of these two enzymes (21, 22). These results indicated that β4GalT-II has specific roles in the biosynthesis of HNK-1 carbohydrate. However, the precise molecular mechanism has not been explored.

Polysialic acid (PSA), a well known neural specific glycan, plays crucial roles in the development of the nervous system, attenuating cellular interactions because of its large and highly negative charge (23, 24). PSA has features in common with HNK-1 in that it is mainly expressed on NCAM and has an *N*-acetyllactosamine residue (Galβ1–4GlcNAc-) in its backbone structure synthesized by β4GalT (25). Surprisingly, however, β4GalT-II-deficient mice as well as β4GalT-I-deficient mice expressed PSA at the same level as wild-type mice (19, 20), indicating the biosynthesis of HNK-1 and PSA to be more complicated mechanisms than was previously thought.

In this study, we demonstrated that β4GalT-II but not β4GalT-I physically interacts with GlcAT-P but not with a polysialyltransferase (PST), which explains the loss of or remaining expression of HNK-1 or PSA in these knock-out mice. Furthermore, overexpression of β4GalT-II enhanced HNK-1 biosynthesis by GlcAT-P compared with β4GalT-I, suggesting that β4GalT-II is specifically required for production of HNK-1.

EXPERIMENTAL PROCEDURES

Materials—The monoclonal antibody (mAb) M6749 against HNK-1 carbohydrate was a gift from Dr. H. Tanaka (Kumamoto University). HNK-1 mAb was purchased from the American Type Culture Collection. The rat anti-mouse NCAM mAb (clone H28) was kindly provided by Dr. K. Ono (Kyoto Prefectural University). RCA120 was purchased from Seikagaku Corp., Tokyo, Japan. The mouse anti-FLAG M2 mAb and rabbit anti-FLAG polyclonal antibody (pAb) were obtained from Sigma. The mouse anti-Myc mAb and rabbit anti-Myc pAb were from Millipore and Abcam, respectively. The rabbit anti-GlcAT-P pAb (GP2) was generated as described previously (16). The mouse anti-GM130 mAb was purchased from BD Biosciences. HRP-conjugated anti-mouse IgG, anti-mouse IgM, anti-rabbit IgG, and anti-rat IgG were obtained from Invitrogen. Protein G-Sepharose TM4 Fast Flow and IgG-Sepharose TM6 Fast Flow were from GE Healthcare. The expression vector pcDNA3.1/myc-His B was from Invitrogen, and p3×FLAG-CMV-10 and p3×FLAG-CMV-14 were from Sigma. The plasmid pEF-BOS was kindly provided by Dr. S. Nagata (Kyoto University).

Mice—β4GalT-I-deficient mice and β4GalT-II-deficient mice were generated as described previously (19, 26). β4GalT-II-deficient mice backcrossed to C57BL/6 mice for more than 10 generations were used for the experiments, whereas β4GalT-I-deficient mice on a mixed background of 129/Sv and C57BL/6 were used because the mice with the C57BL/6 background were lethal.[4] The animal experiments were conducted according to the Fundamental Guidelines for Proper Conduct of Animal Experiments and Related Activities in Academic Research Institutions under the jurisdiction of the Ministry of Education, Culture, Sports, Science and Technology of Japan and approved by the Committees on Animal Experimentation of Kanazawa University and Kyoto University.

Preparation of Brain Homogenate and Membrane Fraction—Whole brains from 4-week-old mice were homogenized with a Polytron homogenizer in 9 volumes of 50 mM Tris-HCl, pH 7.4, containing 150 mM NaCl, 1 mM EDTA, and protease inhibitors (Nacalai Tesque, Kyoto, Japan). The homogenate was centrifuged at 1,000 × *g* for 10 min at 4 °C to remove the nuclei and then centrifuged again at 105,000 × *g* for 1 h at 4 °C. The resulting pellet was used as the membrane fraction.

Peptide N-Glycosidase F Digestion—The membrane fraction of mouse brain was dissolved and denatured with phosphate-buffered saline (PBS) containing 0.5% SDS, 1% 2-mercaptoethanol, and 20 mM EDTA. To reduce the concentration of SDS, the sample was diluted with 4 volumes of PBS containing 0.5% Triton X-100. Two units of peptide *N*-glycosidase F (Roche Applied Science) were added, and the solution was incubated for 16 h at 37 °C.

Expression Plasmids—The subcloning of rat GlcAT-P cDNA into pEF-BOS was performed as described previously (11). The expression plasmid for GlcAT-P-AAA (pEF-BOS/GlcAT-P-AAA) was constructed as reported (16). The mouse β4GalT-I and β4GalT-II coding sequences were amplified by PCR using the primers listed below to create HindIII and EcoRV (skipping stop codon) sites and then cloned into pcDNA3.1/myc-His B. The mouse PST coding sequence was cloned into p3×FLAG-CMV-14 as described previously (16). The expression plasmid for PST-AAA-FLAG (p3×FLAG-CMV-14/PST-AAA) was constructed as follows. p3×FLAG-CMV-14/PST-AER-FLAG was constructed using QuikChange Lightning site-directed mutagenesis kits (Stratagene) according to the manufacturer's directions using the primers listed below, with p3×FLAG-CMV-14/PST-FLAG as a template. Then, p3×FLAG-CMV-14/PST-AAA-FLAG was constructed as mentioned above using the primers listed below, with p3×FLAG-CMV-14/PST-AER-FLAG as a template. cDNAs encoding the Golgi luminal domains of mouse β4GalT-I and -II (from Ser-43 and Asp-33 to the C terminus) were amplified by PCR using the primers listed below and cloned into pEF-BOS-protein A (27), which contains the insulin signal sequence and IgG-binding domain of protein A. For the constructions of prot.A-GalT-Icat and -IIcat, cDNAs encoding the catalytic domains of mouse β4GalT-I and -II (from Leu-128 and Ile-91 to the C terminus) (28) were amplified by PCR using the primers listed below and cloned into pEF-BOS-protein A. pEF-BOS-protein A was digested with SmaI. Then the blunt end fragments of β4GalTs were cloned. GlcAT-P-sol was amplified by PCR using the primers listed

[4] M. Asano and N. Hashimoto, unpublished results.

below with pEF-BOS/GlcAT-P as a template to create EcoRV and NotI sites, and cloned into pEF-1/V5-His A into which the signal sequence of insulin had been inserted between EcoRI and EcoRV sites.

The primers used for β4GalT-I-myc were as follows: GGGAAGCTTGCGGGCCGTCCTCTCAGCCG and TCTCGGTGTCCCGATGTCCACTGTG; β4GalT-II-myc, GGGAAGCTTCTTGCGGGATGAGCAGACTG and GCCTTGAGTGAGCCACGAGA; PST-AER-FLAG, ATGCGCTCAATTGCAGAACGGTGGACCATCTGCACTATAAGTC and GACTTATAGTGCAGATGGTCCACCGTTCTGCAATTGAGCGCAT; PST-AAA-FLAG, ATGCGCTCAATTGCAGCAGCGTGGACCATCTGCACTATAAGTC and GACTTATAGTGCAGATGGTCCACGCTGCTGCAATTGAGCGCAT; prot.A-GalT-I (Ser-43), CTGGCCGCGATCTGAGCCG and CTATCTCGGTGTCCCGATGTCCACT; prot.A-GalT-II (Asp-33), ACGTCTATGCCCAGCACCTGG and TCAGCCTTGAGTGAGCCACGACATG; prot.A-GalT-Icat (Leu-128), TGCCAGCTTGCCCTGAGGAG and CTATCTCGGTGTCCCGATGTCCACT; prot.A-GalT-IIcat (Ile-91), TCATTCCGCCCTGTCCTGAC and TCAGCCTTGAGTGAGCCACGACATG; and GlcAT-P-sol, CCCCGCCATGAGGCACCACC and TGAGCGGCCGCTCAGATCTCCACCGAGGGGT.

Cell Culture and Transfection—N2a cells were cultured in minimum Eagle's medium supplemented with 10% fetal bovine serum at 37 °C until 50–70% confluent. For transfection, cells were plated on 60-mm tissue culture dishes, grown overnight, and then transfected with various expression constructs using FuGENE 6 (Roche Applied Science) according to the manufacturer's directions. Briefly, a 2.5 volume of FuGENE 6 and 1 μg of each DNA were incubated with 100 μl of minimum Eagle's medium for 15 min at room temperature, and then the mixture was added to the tissue culture dishes.

Cell Lysis and Immunoprecipitation of Transiently Expressed Proteins—Cells were collected 24 h after transfection and lysed with a buffer consisting of 20 mM Tris-HCl, pH 7.4, 150 mM NaCl, 1 mM EDTA, 1% Triton X-100, and a protease inhibitor mixture (Nacalai Tesque). After centrifugation, the clarified lysate was incubated with the anti-FLAG rabbit pAb or anti-Myc rabbit pAb for 0.5 h. The mixture was then incubated with protein G-Sepharose TM4 Fast Flow for 2 h with gentle shaking. The beads were precipitated by centrifugation (500 × *g* for 1 min) and washed three times with an excess volume of wash buffer consisting of 20 mM Tris-HCl, pH 7.4, 150 mM NaCl, and 0.1% Tween 20. Proteins bound to the Sepharose beads were eluted by boiling in Laemmli sample buffer.

Immunostaining of N2a Cells—At 24 h post-transfection, cells were washed with PBS, fixed with ice-cold methanol, and incubated with primary antibodies followed by Alexa Fluor-conjugated secondary antibodies (Invitrogen). Cells were visualized with a Fluoview laser confocal microscope system (Olympus).

SDS-PAGE and Western Blot and Lectin Blot Analyses—Proteins were separated by SDS-PAGE with the buffer system of Laemmli and transferred to nitrocellulose membranes. For Western blotting, after being blocked with 5% skim milk in PBS containing 0.05% Tween 20, the membrane was incubated with primary antibodies followed by HRP-conjugated secondary antibodies. For lectin blotting, after being blocked with PBS containing 0.05% Tween 20 (T-PBS), the membrane was incubated with sialidase (Roche Applied Science) according to the manufacturer's instructions, and then incubated with HRP-conjugated lectin in T-PBS. Protein bands were detected with ECL (Pierce) using a LAS3000 Luminoimage analyzer (Fujifilm).

Pulldown Assays—N2a cells were transiently transfected with prot.A-GalT-I (Ser-43), -Icat (Leu-128), -II (Asp-33), or -IIcat (Ile-91) and GlcAT-P-sol. After 6 h of incubation, the culture medium was replaced with serum-free Opti-MEM I (Invitrogen) and incubation continued for another 2 days. Normal human IgG-conjugated Sepharose beads were added to the culture medium containing secreted proteins. The beads were precipitated by centrifugation (500 × *g* for 1 min) and then washed three times with an excess volume of wash buffer consisting of 20 mM Tris-HCl, pH 7.4, 150 mM NaCl, and 0.1% Tween 20. Proteins bound to the Sepharose beads were eluted by boiling in Laemmli sample buffer.

Preparation of Protein A-fused GalTs—COS-1 cells plated on 175-cm^2 tissue culture flasks were transfected with prot.A-GalT-I (Ser-43) or prot.A-GalT-II (Asp-33) using FuGENE 6 transfection reagent. After 5 h of incubation, the culture medium was replaced with serum-free ASF104 medium (Ajinomoto), followed by incubation for another 3 days. Then, the culture medium containing secreted proteins was applied to IgG-Sepharose TM6 fast flow column (GE Healthcare). Unbound proteins were washed out with more than 10 column volumes of PBS. Bound proteins were eluted with 100 mM glycine-HCl, pH 2.5, and then the eluate was immediately neutralized with 3 M Tris-HCl, pH 8.0. The purified prot.A-GalTs were used for the following kinetic analysis of GlcAT-P.

Measurement of Glucuronyltransferase Activity—The FLAG-tagged GlcAT-P catalytic domain (FLAG-P) used was expressed in *Escherichia coli* and purified as described previously (29). The enzymatic activity of GlcAT-P toward glycoprotein acceptors was measured according to the procedure described previously (10) with slight modification. In brief, prior to the assay, FLAG-P (25 ng) was incubated in the absence or presence of prot.A-GalT-I (Ser-43) or prot.A-GalT-II (Asp-33) (100 ng each) at room temperature for 15 min. The preincubated enzyme solution was added to a reaction mixture with a final volume of 25 μl consisting of 200 mM MES, pH 6.5, 0.2% Nonidet P-40, 20 mM $MnCl_2$, 0.1–20 μg ASOR, 100 μM UDP-[^{14}C]GlcA (100,000 dpm), and 0.5 mM ATP. After incubation at 37 °C for 2 h, the assay mixture was spotted onto a Whatman No. 1 filter paper. The filter paper was washed with a 10% (w/v) trichloroacetic acid solution three times, followed by with ethanol/ether (2:1, v/v), and then with ether. The filter paper was air-dried, and then the radioactivity of [^{14}C]GlcA-ASOR was counted with a liquid scintillation counter.

RESULTS

Unaltered Expression of N-Acetyllactosamine on a Major HNK-1 Carrier in β4GalT-II-deficient Mice—Recently, we reported that HNK-1 expression is substantially reduced in β4GalT-II-deficient mice, although an earlier study revealed that β4GalT-I-deficient mice expressed normal levels of

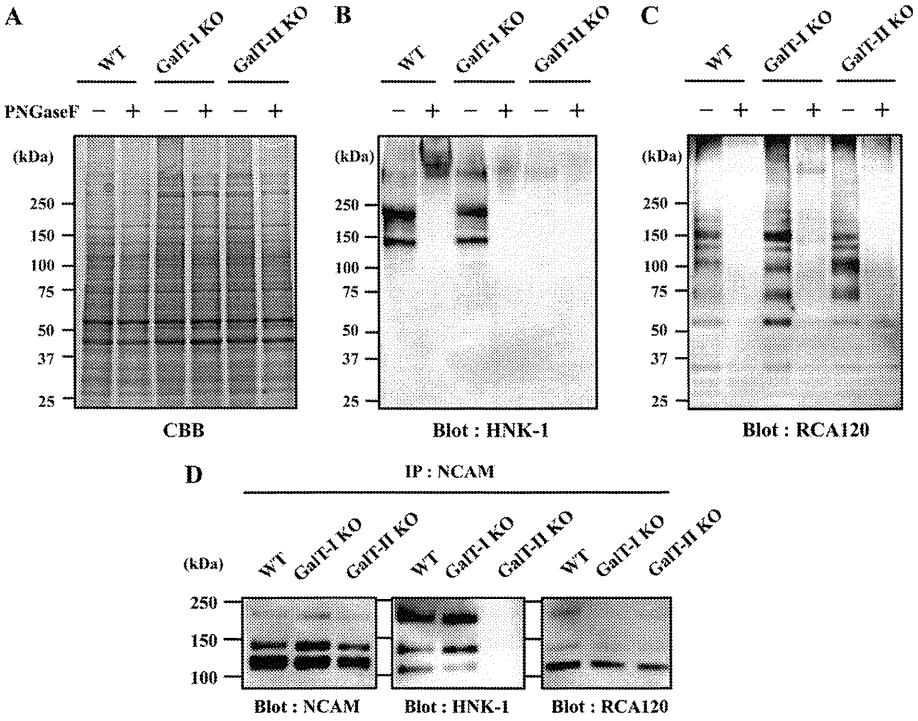

FIGURE 1. **Expression of HNK-1 carbohydrate and *N*-acetyllactosamine in mouse brains.** Membrane fractions of 4-week-old C57BL/6 (WT), β4GalT-I-deficient (GalT-I-KO), and β4GalT-II-deficient (GalT-II-KO) mouse brain were subjected to SDS-PAGE followed by Coomassie Brilliant Blue (*CBB*) staining (*A*), Western blotting with HNK-1 mAb (*B*), or lectin blotting with RCA120 (*C*). *D*, membrane fractions of 4-week-old mouse brains were immunoprecipitated (*IP*) with anti-NCAM antibody, subjected to SDS-PAGE, and blotted with anti-NCAM mAb, HNK-1 mAb, and RCA120. PNGase F, peptide:*N*-glycosidase F.

HNK-1 (19, 20). To directly compare the expression of HNK-1 in these mutant mice, brain membrane fractions were prepared from wild-type and β4GalT-I, II-deficient mice (Fig. 1*A*) and Western-blotted with the HNK-1 mAb (Fig. 1*B*). Consistent with previous reports, HNK-1 expression was dramatically decreased in β4GalT-II-deficient mice but was normal in β4GalT-I-deficient mice. Most HNK-1 epitopes in the wild-type mice disappeared after treatment with peptide *N*-glycosidase F (Fig. 1*B, 2nd lane*), indicating that HNK-1 carbohydrates are mainly expressed on *N*-glycan in the membrane fraction. This suggests that β4GalT-II synthesizes most HNK-1 carbohydrates on *N*-glycans in the brain. To explore the molecular mechanism involved, we first confirmed that the GlcAT-P transcript was expressed normally in these knock-out mice brains (supplemental Fig. 1). Next, to examine whether the *N*-acetyllactosamine residue remains in these knock-out mice, a lectin blot analysis was performed using RCA120, which predominantly recognizes the βGal residue of *N*-acetyllactosamine. Because the nonreducing end of *N*-acetyllactosamine is often capped by sialic acid, the membrane was treated with sialidase prior to RCA120 blotting. As a result, β4GalT-I and -II-deficient mice showed similar reactivity for RCA120 to wild-type mice, most of which disappeared after peptide *N*-glycosidase F treatment, indicating that the *N*-acetyllactosamine on *N*-glycans was normally expressed in these knock-out mice and that several β4GalTs contribute to the biosynthesis of *N*-linked *N*-acetyllactosamine in the brain. This excludes the possibility that the reduction in HNK-1 is due to a general loss of *N*-acetyllactosamine in the β4GalT-II-deficient brain.

Another possibility is that β4GalT-II is the only β4GalT in HNK-1-expressing cell or a specific β4GalT for HNK-1 carrier proteins. To test this, we focused on NCAM. Because NCAM is a major carrier of HNK-1 carbohydrates in the nervous system, it must be expressed in HNK-1-positive cells. NCAM was immunoprecipitated from the brain membrane fraction and blotted with anti-NCAM mAb, HNK-1 mAb, and RCA120. As shown in Fig. 1*D*, three major splicing isoforms of NCAMs (NCAM-120, NCAM-140, and NCAM-180) are detected, and no difference in expression levels of each NCAM isoform (Blot: NCAM) or in reactivity with *Ricinus communis* agglutinin (Blot: *R. communis* agglutinin was observed among three genotypes. In contrast, HNK-1 is predominantly expressed on NCAM-180 and NCAM-140 rather than on NCAM120 in wild-type mice brain, which is consistent with a previous report (30). The HNK-1 on NCAM disappeared in β4GalT-II-deficient mice (Blot: HNK-1). These results indicate that other β4GalTs synthesize *N*-acetyllactosamine even onto NCAM in β4GalT-II-deficient mice and also suggest that β4GalT-II is not the only enzyme in HNK-1-expressing cells and not responsible for the general production of *N*-acetyllactosamine on HNK-1 carrier molecules. Therefore, it is possible that GlcAT-P transfers glucuronic acid (GlcA) only to the *N*-acetyllactosamine structure that β4GalT-II synthesizes, prompting us to speculate that GlcAT-P specifically associates with β4GalT-II.

Co-immunoprecipitation of GlcAT-P and β4GalT-II—To investigate the interaction between β4GalT-II and GlcAT-P, we performed co-immunoprecipitation experiments. Myc-tagged β4GalT-I or -II (β4GalT-I-myc or β4GalT-II-myc) and

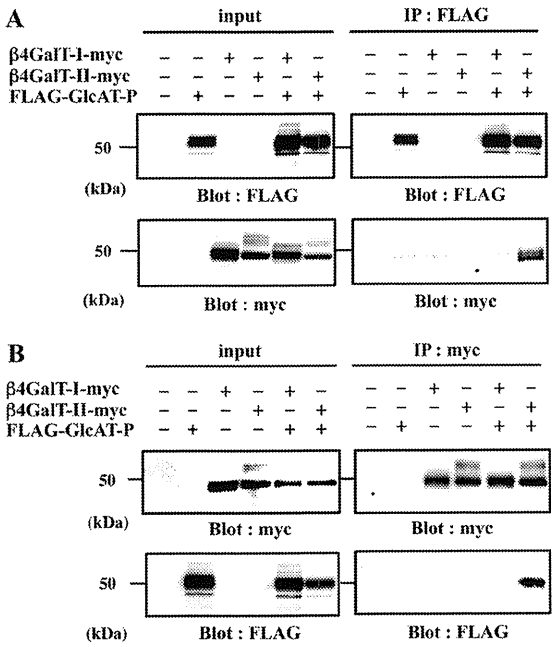

FIGURE 2. **Co-immunoprecipitation of GlcAT-P and β4GalT-II in N2a cells.** Lysate of N2a cells transiently expressing FLAG-GlcAT-P, β4GalT-I-myc, or β4GalT-II-myc was immunoprecipitated (*IP*) with anti-FLAG pAb (*A, IP: FLAG*) or anti-Myc pAb (*B, IP: myc*), subjected to SDS-PAGE, and Western-blotted (*Blot*) with anti-FLAG mAb or anti-Myc mAb. To examine the level of each protein, the cell lysates were directly subjected to SDS-PAGE and Western blotting with anti-FLAG mAb or anti-Myc mAb (*input*).

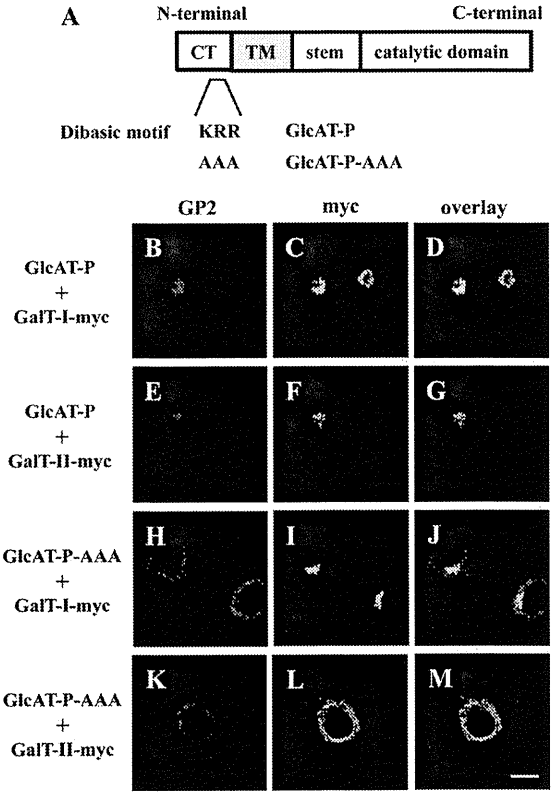

FIGURE 3. **ER retention assays using GlcAT-P-AAA.** *A*, schematic diagrams of GlcAT-P and GlcAT-P-AAA. *CT*, cytoplasmic tail, *TM*, transmembrane domain. *B–M*, N2a cells were transiently co-transfected with GlcAT-P or GlcAT-P-AAA and β4GalT-I-myc or β4GalT-II-myc. GlcAT-P and GlcAT-P-AAA were detected with GP2 pAb (*B, E, H,* and *K*) and Alexa 546-conjugated secondary antibodies. β4GalT-myc (I and II) was detected with anti-Myc mAb (*C, F, I,* and *L*) and Alexa 488-conjugated secondary antibodies. *D, G, J,* and *M*, overlaid images. *Bar*, 10 μm.

FLAG-tagged GlcAT-P (FLAG-GlcAT-P) were transiently expressed in N2a cells, and cell lysates were incubated with anti-FLAG pAb to precipitate FLAG-GlcAT-P (Fig. 2*A*, *IP: FLAG*). Subsequent Western blotting was conducted with anti-Myc mAb to detect β4GalT-I and -II-myc. As shown in Fig. 2*A*, *right lower panel*, β4GalT-II-myc was co-immunoprecipitated by FLAG-GlcAT-P, whereas β4GalT-I-myc was not. To determine whether FLAG-GlcAT-P could be conversely co-precipitated by β4GalT-II-myc, we conducted immunoprecipitation using anti-Myc pAb. As shown in Fig. 2*B*, *right lower panel*, FLAG-GlcAT-P was co-immunoprecipitated by β4GalT-II-myc, but not by β4GalT-I-myc. These results revealed that GlcAT-P specifically interacted with β4GalT-II in cells.

Effect of ER-retained GlcAT-P on β4GalT-II Localization—Next, we performed an ER-retention assay (6, 31) to visualize the interaction. Normally, GlcAT-P and β4GalT-I and -II mainly occur in Golgi, as was confirmed by co-localization with a Golgi marker, GM130, in N2a cells (supplemental Fig. 2). GlcAT-P appeared to co-localize with β4GalT-I as well as β4GalT-II under normal conditions (Fig. 3, *B–G*). In the ER-retention assay, we employed an ER-retained version of GlcAT-P in which a dibasic motif (K/R)(*X*)(K/R) was mutated (Fig. 3*A*). Some glycosyltransferases have this motif in their cytoplasmic tail, which is required for transport from the ER to the Golgi apparatus (32). Actually, GlcAT-P lacking this motif (GlcAT-P-AAA) was retained in the ER (Fig. 3, *H* and *K*, and also see supplemental Fig. 3, *A* and *D*) (16). To investigate the effect of GlcAT-P-AAA on the distribution of β4GalT-I and -II, N2a cells expressing GlcAT-P-AAA and β4GalT-I or -II-myc were immunostained. As a result, the location of β4GalT-II-myc changed to the ER from the Golgi (Fig. 3*L* and supplemental Fig. 3*E*), which overlapped with GlcAT-P-AAA (Fig. 3*M* and supplemental Fig. 3*F*), whereas β4GalT-I-myc was still localized to the Golgi regardless of the expression of GlcAT-P-AAA (Fig. 3, *I* and *J*, and also see supplemental Fig. 3, *B* and *C*). These results reinforce the notion of selective interaction between GlcAT-P and β4GalT-II in cells.

β4GalT-II and β4GalT-I Do Not Associate with PST—To examine the specificity of the binding between β4GalT-II and GlcAT-P, we used a PST instead of GlcAT-P. PST is one of the α2,8-polysialyltransferases involved in the biosynthesis of PSA (33, 34), and PSA is attached to monosialylated *N*-acetyllactosamine on NCAM (35). Our previous study revealed that PSA was expressed in the brain of β4GalT-II-deficient mice at the same level as in wild-type mice (19). This is also the case in β4GalT-I-deficient mice (20). Therefore, we expected that β4GalT-I and -II would not associate with PST. β4GalT-I- or -II-myc and PST-FLAG were expressed in N2a cells, immunoprecipitated with anti-FLAG pAb, and subjected to Western blotting with anti-Myc mAb. As shown in Fig. 4, *lower panel*, β4GalT-I and -II were not co-precipitated with PST, suggesting that these enzymes do not interact in cells.

To support the immunoprecipitation data, an ER retention assay was performed using PST-AAA-FLAG (Fig. 5*A*), a mutant

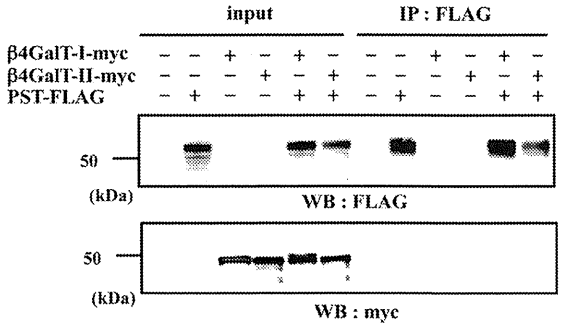

FIGURE 4. **Immunoprecipitation using PST-FLAG and β4GalT-myc in N2a cells.** Lysate of N2a cells transiently expressing PST-FLAG, β4GalT-I-myc, or β4GalT-II-myc were immunoprecipitated (*IP*) with anti-FLAG pAb (*IP: FLAG*), subjected to SDS-PAGE, and Western-blotted with anti-FLAG mAb or anti-Myc mAb. To examine the level of each protein, the cell lysates were directly subjected to SDS-PAGE and then Western blotting (*WB*) with anti-FLAG mAb or anti-Myc mAb (*input*).

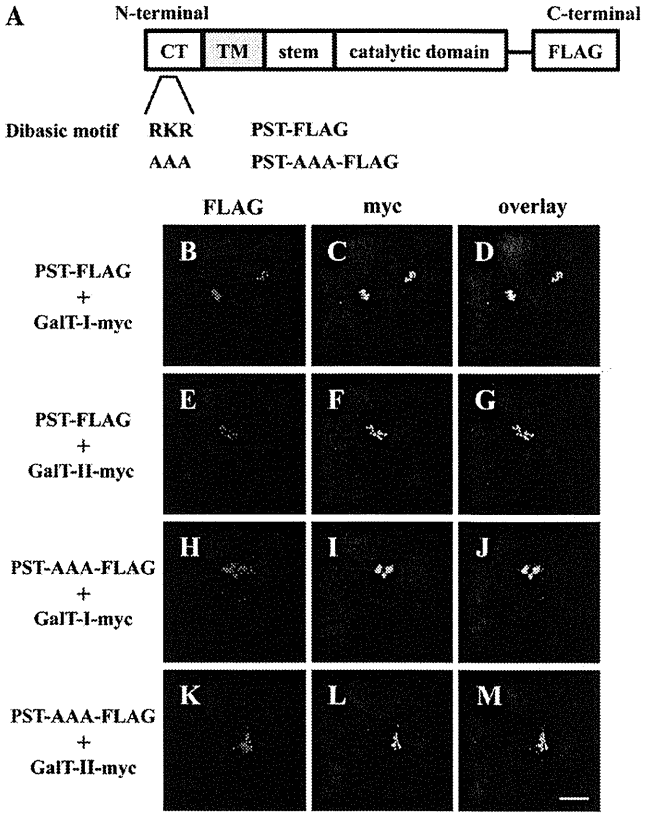

FIGURE 5. **ER retention assays using PST-AAA-FLAG.** *A*, schematic diagrams of PST-FLAG and PST-AAA-FLAG. *B–M*, N2a cells were transiently co-transfected with PST-FLAG or PST-AAA-FLAG and β4GalT-I-myc or β4GalT-II-myc. PST-FLAG or PST-AAA-FLAG was detected with anti-FLAG pAb (*B*, *E*, *H*, and *K*), and Alexa 546-conjugated secondary antibodies. β4GalT-myc (I and II) was detected with anti-Myc mAb (*C*, *F*, *I*, and *L*) and Alexa 488-conjugated secondary antibodies. *D*, *G*, *J*, and *M*, overlaid images. *Bar*, 10 μm. *CT*, cytoplasmic tail, *TM*, transmembrane domain.

of the dibasic motif (K/R)(*X*)(K/R) in PST. PST is also localized to the Golgi apparatus, as confirmed by the co-localization of PST-FLAG with β4GalT-I, and -II-myc in the Golgi (Fig. 5, *B–G*). As expected, the altered distribution of PST-AAA-FLAG was observed as shown in Fig. 5, *H* and *K*, and also in supplemental Fig. 3, *G* and *J*. The distribution of PST-AAA is slightly

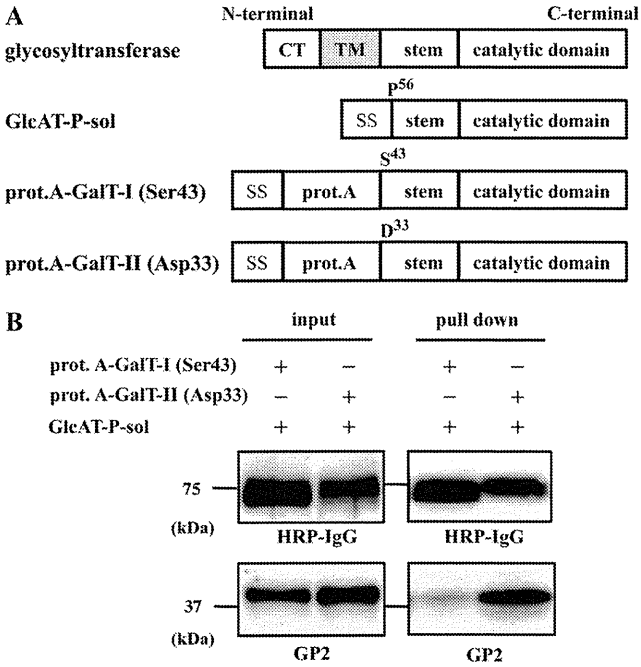

FIGURE 6. **Pulldown assays using soluble forms of GlcAT-P-sol, prot.A-GalT-I, and prot.A-GalT-II.** *A*, schematic diagrams of GlcAT-P-sol, prot.A-GalT-I (Ser-43), and prot.A-GalT-II (Asp-33). *SS*, signal sequence. *B*, culture medium of N2a cells transiently expressing GlcAT-P-sol and prot.A-GalT-I (Ser-43) or prot.A-GalT-II (Asp-33) was incubated with IgG-Sepharose TM6 Fast Flow (pulldown), subjected to SDS-PAGE, and Western-blotted with HRP-conjugated normal rabbit IgG or GP2 pAb. To examine the level of each protein, the culture medium was directly subjected to SDS-PAGE and then Western-blotted with HRP-conjugated normal rabbit IgG or GP2 pAb (*input*). *CT*, cytoplasmic tail, *TM*, transmembrane domain.

different from GlcAT-P-AAA, *i.e.* PST-AAA was detected not only in ER but in Golgi, suggesting that the effect of the mutation of dibasic motif on ER distribution varies by an individual glycosyltransferase as described previously (32). However, the altered distribution of PST-AAA did not perturb the Golgi-based localization of β4GalT-I and -II-myc (Fig. 5, *I*, *J*, *L*, and *M*, and also see supplemental Fig. 3, *H*, *I*, *K*, and *L*). These results revealed that β4GalT-I and -II do not associate with PST, supporting our idea that β4GalT-II and GlcAT-P form a specific complex.

Interaction between GlcAT-P and β4GalT-II through Their Luminal Domains—Glycosyltransferases, such as GlcAT-P and β4GalT, are type II transmembrane proteins with a short cytoplasmic tail, a hydrophobic single-pass transmembrane domain, a stem region, and a catalytic domain (Fig. 6*A*) (36). We previously reported that GlcAT-P and HNK-1ST formed an enzyme complex through their catalytic domains in the Golgi lumen (37). Thus, we examined whether GlcAT-P and β4GalT-II also form a complex via their Golgi luminal domains. We constructed an expression vector encoding the luminal domain of GlcAT-P downstream of the insulin signal sequence (GlcAT-P-sol). Similarly, expression vectors for luminal domains of β4GalT-I and -II fused with the signal sequence and protein A (prot.A-GalT-I (Ser-43) and prot.A-GalT-II (Asp-33), respectively) were constructed (Fig. 6*A*). The culture medium of N2a cells expressing GlcAT-P-sol and prot.A-GalT-I (Ser-43) or -II (Asp-33) was incubated with IgG-Sephar-

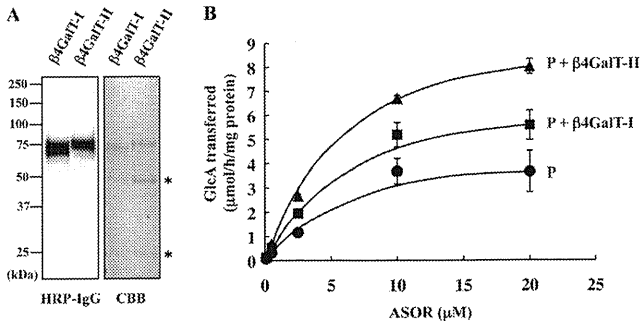

FIGURE 7. **Effect of the co-presence of β4GalT-II on the *in vitro* glucuronyltransferase reaction of GlcAT-P.** *A*, prot.A-GalT-I (Ser-43) (β4GalT-I) or -II (Asp-33) (β4GalT-II) was expressed in COS-1 cells and purified from the culture media. The purified enzymes were subjected to Western blotting with HRP-conjugated rabbit IgG and Coomassie Brilliant Blue (*CBB*) staining. *Asterisks* indicate heavy and light chains of immunoglobulin derived from human IgG Sepharose. *B*, rate of glucuronyltransferase reaction of FLAG-P was measured in the absence of β4GalTs (P), or in the presence of prot.A-GalT-I (Ser-43) (*P + β4GalT-I*) or prot.A-GalT-II (Asp-33) (*P + β4GalT-II*) using different concentrations of ASOR as substrates. All experiments were employed in triplicate, and *error bars* indicate S.E.

ose beads to pull down the prot.A-tagged enzymes. Subsequent Western blotting was conducted with HRP-conjugated IgG and anti-GlcAT-P pAb (GP2) to detect prot.A-fused enzymes and GlcAT-P, respectively. As shown in Fig. 6*B*, GlcAT-P-sol was highly co-precipitated with prot.A-GalT-II compared with prot.A-GalT-I, indicating that Golgi luminal domains are enough to form the enzyme complex. To narrow down the binding region of Golgi luminal domains of β4GalTs, we also constructed expression vectors for catalytic domains of β4GalT-I and -II fused with the signal sequence and protein A (prot.A-GalT-Icat (Leu-129) and prot.A-GalT-IIcat (Ile-91), respectively) and performed pulldown assay as described above. However, neither prot.A-GalT-Icat (Leu-129) nor prot.A-GalT-IIcat (Ile-91) interacts with GlcAT-P-sol (data not shown), suggesting that the deleted stem region are necessary for the specific binding of GlcAT-P and β4GalT-II. Therefore, prot.A-GalT-I (Ser-43) and prot.A-GalT-II (Asp-33) were used for the following kinetic analysis of GlcAT-P.

Kinetic Analysis of GlcAT-P—Next, to investigate whether or not a specific association of β4GalT-II affects GlcAT-P activity, we examined the dependence of the rate of the glucuronyltransferase reaction on the concentration of ASOR as a glycoprotein acceptor in the presence or absence of β4GalT-I or β4GalT-II. For this kinetic analysis, we used FLAG-tagged human GlcAT-P (from Thr-58 to the C terminus, FLAG-P) expressed in *E. coli*. The method for expression and purification of FLAG-P had been already established (29). Human GlcAT-P is highly homologous to mouse GlcAT-P, especially 99.3% of amino acids are identical in the region we used (Thr-58 to C terminus). prot.A-GalT-I (Ser-43) and prot.A-GalT-II (Asp-33) were purified from culture media of COS-1 cells that had been transfected with their expression vectors as shown in Fig. 7*A*. The rate of glucuronyltransferase reaction of FLAG-P in the absence of prot.A-GalTs was compared with that in the presence of prot.A-GalT-I (Ser-43) or prot.A-GalT-II (Asp-33) using different concentrations of ASOR. As shown in Fig. 7*B*, the rate of FLAG-P reaction was increased depending on the concentration of ASOR and enhanced in the presence of GalT-I

TABLE 1
Kinetic parameters of GlcAT-P

	K_m	V_{max}	k_{cat}	k_{cat}/K_m	Relative k_{cat}/K_m
	μM	μmol/h/mg	s^{-1}	$\mu M^{-1} s^{-1}$	*-fold*
GlcAT-P	7.46	4.90	0.0545	7.30	1
GlcAT-P + β4GalT-I	6.62	7.53	0.0837	12.6	1.73
GlcAT-P + β4GalT-II	6.09	9.86	0.110	18.0	2.47

or -II. The data were analyzed by means of Lineweaver-Burk plotting, and the kinetic parameters were then determined (Table 1). Apparent V_{max} value was increased about 2-fold, and the apparent K_m value was slightly decreased by β4GalT-II. Thus, β4GalT-II resulted in an approximate 2.5-fold increase in the catalytic efficiency k_{cat}/K_m of FLAG-P. To our surprise, β4GalT-I, which does not associate with GlcAT-P, also enhanced the catalytic efficiency k_{cat}/K_m about 1.7-fold. However, the catalytic efficiency in the presence of β4GalT-II is still higher than that of β4GalT-I. These results suggest that the enzyme complex of GlcAT-P and β4GalT-II is indeed capable of facilitating the expression of HNK-1.

Enhanced HNK-1 Biosynthesis by Enzyme Complex in N2a Cells—To determine the effect of the interaction on HNK-1 carbohydrate production in cells, a Western blot analysis was performed with the M6749 mAb. This mAb recognizes nonsulfated HNK-1 carbohydrate (GlcAβ1–3Galβ1–4GlcNAc) (38), and N2a cells do not express endogenous GlcAT-P or HNK-1 carbohydrate (Fig. 8*A*, *1st lane*). By employing this antibody, we can examine the level of nonsulfated HNK-1 carbohydrate, which was produced by GlcAT-P (Fig. 8*A*, *2nd lane*). GlcAT-P and β4GalT-I or -II-myc were co-expressed in N2a cells, and then cell lysates were subjected to SDS-PAGE and Western-blotted with the M6749 mAb, GP2 pAb, and anti-Myc mAb. As shown in Fig. 8*A*, M6749 immunoreactivity was increased when co-expressed with β4GalT-I and -II-myc despite the comparable expression of GlcAT-P (compare *2nd lane* with *3rd* and *4th lanes*), probably because of the increased amount of *N*-acetyllactosamine, which can be utilized as an acceptor by GlcAT-P. Intriguingly, however, M6749 immunoreactivity was increased more when GlcAT-P was co-expressed with β4GalT-II-myc than with β4GalT-I-myc (Fig. 8*A*, compare *3rd* with *4th lane*). To confirm these results, we quantitated two bands (see Fig. 8*A*, *band 1* and *2*) by means of densitometric analysis using image analysis software ImageGauge (FujiFilm). As shown in Table 2, co-expression of GlcAT-P and β4GalT-II-myc caused about 3-fold (see Fig. 8*A*, *bands 1* and *2*) increases in M6749 immunoreactivity compared with that of GlcAT-P, and a 2-(*band 1*) or 1.4-fold (*band 2*) increase compared with that of GlcAT-P and β4GalT-I-myc. These suggest that β4GalT-II is better able to promote HNK-1 biosynthesis by associating with GlcAT-P. We carried out a similar analysis with immunoprecipitated NCAM, which is endogenously expressed in N2a cells. As shown in Fig. 8*B*, the highest expression of the M6749 epitope was observed when GlcAT-P was co-expressed with β4GalT-II-myc. These results suggest that the complex of GlcAT-P and β4GalT-II contributes to the enhancement of HNK-1 synthesis.

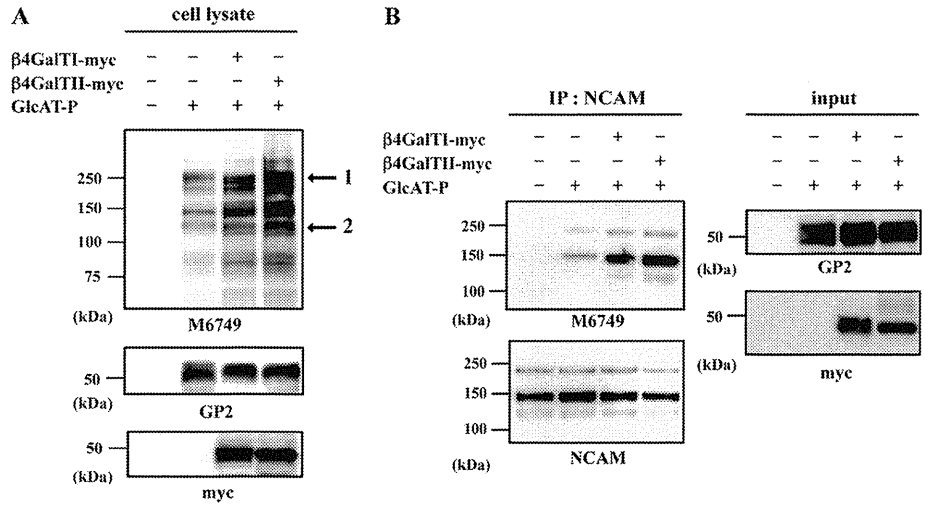

FIGURE 8. **Effect of the enzyme complex on HNK-1 expression in N2a cells.** *A*, lysates of N2a cells transiently expressing GlcAT-P, β4GalT-I-myc, or β4GalT-II-myc were subjected to SDS-PAGE and then Western blotted with M6749 mAb, GP2 pAb, or anti-Myc mAb. *Arrows* indicate bands used for quantification by densitometric analyses. *B*, lysates of N2a cells transiently expressing GlcAT-P and β4GalT-I-myc or β4GalT-II-myc were immunoprecipitated (*IP*) with anti-NCAM mAb and subjected to SDS-PAGE and then Western-blotted with M6749 mAb or anti-NCAM mAb.

TABLE 2
Quantitative analysis of the effect of the enzyme complex

	Mock	GlcAT-P	GlcAT-P + β4GalT-I-myc	GlcAT-P + β4GalT-II-myc
Band 1				
Intensity (a.u.)[a]	0	0.48	0.77	1.53
-Fold		1.00	1.60	3.20
Band 2				
Intensity (a.u.)	0	0.21	0.43	0.60
-Fold		1.00	2.03	2.86

[a] The immunoreactivity with M6749 mAb was calculated and normalized to GlcAT-P expression and is shown as intensity in arbitrary units (a.u.).

DISCUSSION

The β4GalT family has seven members, but the biological roles have not been fully understood. We recently reported that β4GalT-II-deficient mice showed a marked reduction in levels of HNK-1 carbohydrate and impaired spatial memory, and the phenotypes are similar to those of GlcAT-P-deficient mice (19). Moreover, β4GalT-II is highly expressed in the brain although β4GalT-I is ubiquitous (39). These findings suggest intrinsic roles *in vivo*, although β4GalT-I and -II show the highest sequence similarity among β4GalTs. Analyses using these gene-deficient mice revealed that β4GalT-II is crucial to the production of HNK-1, but the underlying mechanism was not elucidated. In this study, we produced evidence that β4GalT-II physically associates with GlcAT-P (Figs. 2 and 3) probably through the luminal stem domain of β4GalT-II. Considering the similar domain organizations and molecular sizes of GlcAT-P and β4GalT-II, the stem domain of GlcAT-P may also be involved in this interaction. Because we had revealed that GlcAT-P bound to HNK-1ST through the catalytic region (37), β4GalT-II seems not to compete with HNK-1ST for the binding to GlcAT-P; rather, these three enzymes may simultaneously form a large functional complex to synthesize HNK-1 efficiently in living cells. Actually, we revealed that β4GalT-II is capable of increasing the catalytic efficiency k_{cat}/K_m of the GlcAT-P catalytic reaction using *in vitro* enzyme assay system (Fig. 7). Also in N2a cells, the co-expression of β4GalT-II and GlcAT-P enhanced HNK-1 biosynthesis (Fig. 8). These results suggest that HNK-1 expression is regulated by the interaction of these two enzymes.

We found that both β4GalT-I- and -II-deficient mice showed normal levels of *N*-acetyllactosamine on *N*-glycans, indicating that several β4GalTs actually contribute to galactosylation in the brain. The specific loss of HNK-1 in β4GalT-II-deficient mice can be explained in several ways. The present analysis suggests that β4GalT-II is not the only enzyme for *N*-acetyllactosamine synthesis in HNK-1-expressing cells because *N*-acetyllactosamine is likely expressed at normal levels in β4GalT-II knock-out mice even on NCAM. Our experiment showed that β4GalT-II does not specialize in the galactosylation of HNK-1-expressing molecules such as NCAM by recognizing their polypeptide backbones, because the galactosylation of NCAM is unlikely to be impaired in β4GalT-II knock-out mice. β4GalT-II might act on a specific *N*-glycosylation site or specific branch of *N*-glycan that is preferentially modified further by GlcAT-P. We demonstrated here that simply the presence of *N*-acetyllactosamine or GlcAT-P is not sufficient for HNK-1 biosynthesis and that both *N*-acetyllactosamines synthesized by β4GalT-II and GlcAT-P are required. Although β4GalT-II is involved in HNK-1 biosynthesis, this enzyme is not a chaperone-like molecule for GlcAT-P, because a recombinant GlcAT-P from *E. coli* was fully active without β4GalT-II *in vitro* (29). Rather, we speculate that β4GalT-II would be in a specialized complex with GlcAT-P in a specific Golgi compartment to cooperatively catalyze their transfer reactions for HNK-1 synthesis on specific glycoproteins.

To our surprise, β4GalT-I also had the potential to activate HNK-1 biosynthesis (Fig. 8), even though its effect was weaker than β4GalT-II. This result could be explained by the overproduction of *N*-acetyllactosamine residues by β4GalT-I overexpression even without enzyme-enzyme interaction. Meanwhile, our *in vitro* analysis also showed that β4GalT-I weakly activated GlcAT-P catalytic activity (Fig. 7). Although we could not detect the interaction between GlcAT-P and β4GalT-I in

cell-based co-immunoprecipitation assays, weaker binding was observed in pulldown assays (Fig. 6*B*). These results suggest that β4GalT-I could compensate for the loss of HNK-1 biosynthesis in β4GalT-II-deficient cells if it could be overexpressed. Because HNK-1 expression almost disappeared in the β4GalT-II-deficient brain, it suggests that the levels of other β4GalTs in HNK-1-expressing cells may be under the levels that are required for compensation for the loss of β4GalT-II.

We previously reported that β4GalT-I- and -II-deficient mice showed the same level of PSA expression as wild-type mice, indicating that the biosynthesis of PSA does not depend on these enzymes (19, 20). Also, we found that PST does not associate with β4GalT-I or -II (Fig. 4). Regarding the biosynthesis of PSA, another β4GalT may be associated with polysialyltransferase to specifically synthesize the inner structure of PSA. Alternatively, polysialyltransferase may not distinguish between the inner *N*-acetyllactosamines synthesized by several β4GalTs. Other β4GalTs could compensate for the loss of deficiency of a given β4GalT. Moreover, acidic amino acid residues in the fibronectin type III domain adjacent to the fifth Ig domain of NCAM, which has *N*-glycosylation sites attaching to PSA, were reported to be required for polysialylation (40). PSA biosynthesis would be mainly dependent on the polypeptide backbone of NCAM rather than the enzyme responsible for production of the inner *N*-acetyllactosamine. It is indicated that the biosynthesis of PSA is considerably different from that of HNK-1, despite some common features between these two neural glycans expressed on NCAM.

In recent years, many groups have reported that enzyme complexes of glycosyltransferases have enhanced catalytic activities. Seko and Yamashita (5) showed that a complex of β3GnT2 and β3GnT8 produced more poly-*N*-acetyllactosamine. Our previous study demonstrated that GlcAT-P interacts with HNK-1ST, and the interaction enhances the enzymatic activity of HNK-1ST (37). Also, it has been reported that the activities of some glycosyltransferases are regulated through interaction with nonglycosyltransferases. For example, GnT-I activity was inhibited by interaction with GnT-I-IP (GnT-I inhibitory protein), resulting in the expression of high mannose-type *N*-glycans during spermatogenesis (41). T-synthase (C1β3Gal-T) forms a complex with core 1 β3GalT-specific molecular chaperone, which functions as a specific chaperone. Core 1 β3GalT-specific molecular chaperone is essential for the T-synthase activity and synthesizing T-antigen (42). Actually, core 1 β3GalT-specific molecular chaperone is a factor responsible for Tn syndrome, a genetic disease involving a deficiency in T-antigen but no defect in T-synthase (43). In this study, we found that HNK-1 expression is not regulated simply by GlcAT-P but also by the interaction of the enzymes. Supporting this finding, the distribution of GlcAT-P mRNA did not completely match the pattern of HNK-1 expression in the brain. For example, HNK-1 antibody staining showed parasagittal stripes in the molecular layer in the cerebellum (44) because of HNK-1 carbohydrate expression on a limited population of Purkinje cells, whereas GlcAT-P mRNA is likely expressed in most Purkinje cells (45). It would be of interest to compare the distribution of β4GalT-II mRNA and HNK-1 carbohydrate in the brain. Taken together, to understand the precise mechanisms of expression and proper functions of glycans, it is important to recognize that many glycosyltransferases form complexes *in vivo*.

HNK-1 carbohydrate has an important role in synaptic plasticity and spine morphogenesis in the nervous system (14, 15). These functions are based on its specific expression on certain carriers such as NCAM and GluR2, which is a subunit of the α-amino-3-hydroxy-5-methylisoxazole propionate-type glutamate receptor. It should be noted that another subunit, GluR1, which forms a complex with GluR2 to make a functional α-amino-3-hydroxy-5-methylisoxazole propionate receptor *in vivo*, is not modified with HNK-1 (46) even if several complex-type *N*-glycans are expressed on GluR1. This indicates that HNK-1 carbohydrate greatly contributes to the specific function of GluR2, but the underlying mechanism of this selective modification is poorly understood. It could be involved in the selective modification to form the complex of β4GalT-II and GlcAT-P. As well as HNK-1 carbohydrate, many glycans are expressed on specific target proteins, thereby regulating their functions. Thus, it is of great interest to study the mechanisms by which the functions of individual glycosyltransferases are regulated to produce glycoconjugates.

REFERENCES

1. Ohtsubo, K., and Marth, J. D. (2006) *Cell* **126,** 855–867
2. Lowe, J. B., and Marth, J. D. (2003) *Annu. Rev. Biochem.* **72,** 643–691
3. Sugimoto, I., Futakawa, S., Oka, R., Ogawa, K., Marth, J. D., Miyoshi, E., Taniguchi, N., Hashimoto, Y., and Kitazume, S. (2007) *J. Biol. Chem.* **282,** 34896–34903
4. Seko, A. (2006) *Trends Glycosci. Glycotechnol.* **18,** 209–230
5. Seko, A., and Yamashita, K. (2008) *J. Biol. Chem.* **283,** 33094–33100
6. Lee, P. L., Kohler, J. J., and Pfeffer, S. R. (2009) *Glycobiology* **19,** 655–664
7. Schwarting, G. A., Jungalwala, F. B., Chou, D. K., Boyer, A. M., and Yamamoto, M. (1987) *Dev. Biol.* **120,** 65–76
8. Yoshihara, Y., Oka, S., Watanabe, Y., and Mori, K. (1991) *J. Cell Biol.* **115,** 731–744
9. Voshol, H., van Zuylen, C. W., Orberger, G., Vliegenthart, J. F., and Schachner, M. (1996) *J. Biol. Chem.* **271,** 22957–22960
10. Oka, S., Terayama, K., Kawashima, C., and Kawasaki, T. (1992) *J. Biol. Chem.* **267,** 22711–22714
11. Terayama, K., Oka, S., Seiki, T., Miki, Y., Nakamura, A., Kozutsumi, Y., Takio, K., and Kawasaki, T. (1997) *Proc. Natl. Acad. Sci. U.S.A.* **94,** 6093–6098
12. Seiki, T., Oka, S., Terayama, K., Imiya, K., and Kawasaki, T. (1999) *Biochem. Biophys. Res. Commun.* **255,** 182–187
13. Bakker, H., Friedmann, I., Oka, S., Kawasaki, T., Nifant'ev, N., Schachner, M., and Mantei, N. (1997) *J. Biol. Chem.* **272,** 29942–29946
14. Yamamoto, S., Oka, S., Inoue, M., Shimuta, M., Manabe, T., Takahashi, H., Miyamoto, M., Asano, M., Sakagami, J., Sudo, K., Iwakura, Y., Ono, K., and Kawasaki, T. (2002) *J. Biol. Chem.* **277,** 27227–27231
15. Morita, I., Kakuda, S., Takeuchi, Y., Kawasaki, T., and Oka, S. (2009) *Neuroscience* **164,** 1685–1694
16. Kizuka, Y., Tonoyama, Y., and Oka, S. (2009) *J. Biol. Chem.* **284,** 9247–9256
17. Lo, N. W., Shaper, J. H., Pevsner, J., and Shaper, N. L. (1998) *Glycobiology* **8,** 517–526
18. Hennet, T. (2002) *Cell. Mol. Life Sci.* **59,** 1081–1095
19. Yoshihara, T., Sugihara, K., Kizuka, Y., Oka, S., and Asano, M. (2009) *J. Biol. Chem.* **284,** 12550–12561
20. Kido, M., Asano, M., Iwakura, Y., Ichinose, M., Miki, K., and Furukawa, K. (1998) *Biochem. Biophys. Res. Commun.* **245,** 860–864
21. Almeida, R., Amado, M., David, L., Levery, S. B., Holmes, E. H., Merkx, G., van Kessel, A. G., Rygaard, E., Hassan, H., Bennett, E., and Clausen, H. (1997) *J. Biol. Chem.* **272,** 31979–31991

22. Guo, S., Sato, T., Shirane, K., and Furukawa, K. (2001) *Glycobiology* **11,** 813–820
23. Rutishauser, U. (2008) *Nat. Rev. Neurosci.* **9,** 26–35
24. Mühlenhoff, M., Eckhardt, M., and Gerardy-Schahn, R. (1998) *Curr. Opin. Struct. Biol.* **8,** 558–564
25. Kudo, M., Kitajima, K., Inoue, S., Shiokawa, K., Morris, H. R., Dell, A., and Inoue, Y. (1996) *J. Biol. Chem.* **271,** 32667–32677
26. Asano, M., Furukawa, K., Kido, M., Matsumoto, S., Umesaki, Y., Kochibe, N., and Iwakura, Y. (1997) *EMBO J.* **16,** 1850–1857
27. Kakuda, S., Sato, Y., Tonoyama, Y., Oka, S., and Kawasaki, T. (2005) *Glycobiology* **15,** 203–210
28. Qasba, P. K., Ramakrishnan, B., and Boeggeman, E. (2008) *Curr. Drug Targets* **9,** 292–309
29. Kakuda, S., Oka, S., and Kawasaki, T. (2004) *Protein Expr. Purif.* **35,** 111–119
30. Kruse, J., Mailhammer, R., Wernecke, H., Faissner, A., Sommer, I., Goridis, C., and Schachner, M. (1984) *Nature* **311,** 153–155
31. Nilsson, T., Hoe, M. H., Slusarewicz, P., Rabouille, C., Watson, R., Hunte, F., Watzele, G., Berger, E. G., and Warren, G. (1994) *EMBO J.* **13,** 562–574
32. Giraudo, C. G., and Maccioni, H. J. (2003) *Mol. Biol. Cell* **14,** 3753–3766
33. Eckhardt, M., Mühlenhoff, M., Bethe, A., Koopman, J., Frosch, M., and Gerardy-Schahn, R. (1995) *Nature* **373,** 715–718
34. Kojima, N., Yoshida, Y., and Tsuji, S. (1995) *FEBS Lett.* **373,** 119–122
35. Nakayama, J., and Fukuda, M. (1996) *J. Biol. Chem.* **271,** 1829–1832
36. Breton, C., Mucha, J., and Jeanneau, C. (2001) *Biochimie* **83,** 713–718
37. Kizuka, Y., Matsui, T., Takematsu, H., Kozutsumi, Y., Kawasaki, T., and Oka, S. (2006) *J. Biol. Chem.* **281,** 13644–13651
38. Tagawa, H., Kizuka, Y., Ikeda, T., Itoh, S., Kawasaki, N., Kurihara, H., Onozato, M. L., Tojo, A., Sakai, T., Kawasaki, T., and Oka, S. (2005) *J. Biol. Chem.* **280,** 23876–23883
39. Nakamura, N., Yamakawa, N., Sato, T., Tojo, H., Tachi, C., and Furukawa, K. (2001) *J. Neurochem.* **76,** 29–38
40. Mendiratta, S. S., Sekulic, N., Lavie, A., and Colley, K. J. (2005) *J. Biol. Chem.* **280,** 32340–32348
41. Huang, H. H., and Stanley, P. (2010) *J. Cell Biol.* **190,** 893–910
42. Ju, T., and Cummings, R. D. (2002) *Proc. Natl. Acad. Sci. U.S.A.* **99,** 16613–16618
43. Ju, T., and Cummings, R. D. (2005) *Nature* **437,** 1252
44. Marzban, H., Sillitoe, R. V., Hoy, M., Chung, S. H., Rafuse, V. F., and Hawkes, R. (2004) *J. Neurocytol.* **33,** 117–130
45. Inoue, M., Kato, K., Matsuhashi, H., Kizuka, Y., Kawasaki, T., and Oka, S. (2007) *Brain Res.* **1179,** 1–15
46. Morita, I., Kakuda, S., Takeuchi, Y., Itoh, S., Kawasaki, N., Kizuka, Y., Kawasaki, T., and Oka, S. (2009) *J. Biol. Chem.* **284,** 30209–30217

Biochemical and Biophysical Research Communications 415 (2011) 109–113

Contents lists available at SciVerse ScienceDirect

Biochemical and Biophysical Research Communications

journal homepage: www.elsevier.com/locate/ybbrc

Sulfation of glucuronic acid in the linkage tetrasaccharide by HNK-1 sulfotransferase is an inhibitory signal for the expression of a chondroitin sulfate chain on thrombomodulin

Naoki Nakagawa [a], Tomomi Izumikawa [b], Hiroshi Kitagawa [b], Shogo Oka [a,*]

[a] Department of Biological Chemistry, Human Health Sciences, Graduate School of Medicine, Kyoto University, Kyoto 606-8507, Japan
[b] Department of Biochemistry, Kobe Pharmaceutical University, Kobe 658-8558, Japan

ARTICLE INFO

Article history:
Received 30 September 2011
Available online 12 October 2011

Keywords:
HNK-1 carbohydrate epitope
Thrombomodulin
HNK-1ST
GAG-protein linkage region
Anti-coagulant activity

ABSTRACT

HNK-1 (human natural killer-1) carbohydrate epitope (HSO_3-3GlcAβ1-3Galβ1-4GlcNAc-) recognized by a HNK-1 monoclonal antibody is highly expressed in the nervous system and biosynthesized by a glucuronyltransferase (GlcAT-P or GlcAT-S), and sulfotransferase (HNK-1ST). A similar oligosaccharide (HSO_3-3GlcAβ1-3Galβ1-3Galβ1-4Xyl) also recognized by the HNK-1 antibody had been found in a glycosaminoglycan (GAG)-protein linkage region of α-thrombomodulin (TM) from human urine. However, which sulfotransferase is involved in sulfation of the terminal GlcA in the GAG-protein linkage region remains unclear. In this study, using CHO-K1 cells in which neither GlcAT-P nor GlcAT-S is endogenously expressed, we found that HNK-1ST has the ability to produce HNK-1 immunoreactivity on α-TM. We also demonstrated that HNK-1ST caused the suppression of chondroitin sulfate (CS) synthesis on TM and a reduction of its anti-coagulant activity. Moreover, using an *in vitro* enzyme assay system, the HNK-1-positive TM was found not to be utilized as a substrate for CS-polymerizing enzymes (chondroitin synthase (ChSy) and chondroitin polymerizing factor (ChPF)). These results suggest that HNK-1ST is involved in 3-*O*-sulfation of the terminal GlcA of the linkage tetrasaccharide which acts as an inhibitory signal for the initiation of CS biosynthesis on TM.

1. Introduction

Proteoglycans (PGs) ubiquitously expressed on the cell surface and in the extracellular matrix, are physiologically essential macromolecules modified by glycosaminoglycan (GAG) sidechains including chondroitin sulfate (CS) and heparan sulfate (HS). GAGs have a linear polysaccharide structure comprised of repeating disaccharide units, [(-4GlcAβ1-3GalNAcβ1-)$_n$] for CS and [(-4GlcAβ1-4GlcNAcα1-)$_n$] for HS [1]. The polymerization of GAGs is triggered by the first transfer reaction of GalNAc or GlcNAc to the non-reducing terminus of the GAG-protein linkage tetrasaccharide, GlcAβ1-3Galβ1-3Galβ1-4Xyl-*O*-Ser [1]. This unique tetrasaccharide is generated by xylosyltransferase (XylT), galactosyl transferase (GalT)-I, GalT-II, and glucuronyltransferase I (GlcAT-I) [1–6]. GAGs attached to a protein core are further processed by modifications such as sulfation and epimerization to various degrees dependent on tissue type or developmental stage, generating fully functional PGs [7,8].

Thrombomodulin (TM), a cell surface PG, is a critical mediator of endothelial anti-coagulant defenses occurring as both a CS-PG (β-TM) and a protein (α-TM) unsubstituted by CS, hence its description as a "part-time" PG [9]. Studies on the anti-coagulant effects of TM demonstrated that it has cofactor activity for thrombin-dependent activation of protein C, direct inhibition of fibrinogen cleavage by thrombin, and indirect enhancement of the association of antithrombin III with thrombin [10]. We previously demonstrated that a recombinant human α-TM expressed in CHO-K1 cells bore a truncated un-modified tetrasaccharide linkage structure [11]. Comparative studies on the anti-coagulant effects of α-TM and β-TM revealed that the CS chain of TM plays an important role in regulating the anti-coagulative functions [12]. Thus, it is important to investigate a possible biosynthetic mechanism for part-time PGs.

Human natural killer-1 (HNK-1), a neural carbohydrate epitope abundantly expressed during the brain development, is required for the acquisition of higher-order brain functions including synaptic plasticity [13–15]. A structural feature of this epitope is the terminal sulfated glucuronic acid. Therefore, glucuronyltransferase (GlcAT-P or GlcAT-S) and HNK-1 sulfotransferase (HNK-1ST) are key enzymes for HNK-1 biosynthesis. We demonstrated that GlcAT-P (also GlcAT-S) and HNK-1ST specifically interact and form an enzyme complex effective of HNK-1 biosynthesis [16]. Intrigu

* Corresponding author. Address: Kawahara-cho 53, shogoin, Sakyo-ku, Kyoto 606-8507, Japan. Fax: +81 75 751 3959.
E-mail address: shogo@hs.med.kyoto-u.ac.jp (S. Oka).

0006-291X/$ - see front matter © 2011 Elsevier Inc. All rights reserved.
doi:10.1016/j.bbrc.2011.10.023

ingly, we also found that HNK-1ST interacts with GlcAT-I, implying a physiological role for this association [16]. In addition, 3-*O*-sulfation of the terminal GlcA of the linkage tetrasaccharide was identified in α-TM isolated from human urine and this structure was recognized by a HNK-1 monoclonal antibody (mAb) [17]. These findings, led us to the hypothesis that HNK-1ST is the sulfotransferase responsible for the terminal 3-*O*-sulfation of the linkage region. In this regard, recent studies identified various modifications of the linkage tetrasaccharide and revealed their effects on GAG biosynthesis, providing important clues as to the biosynthetic mechanism of GAG. For instance, 2-*O*-phosphorylation of xylose positively affects GlcAT-I activity, facilitating the linkage tetrasaccharide synthesis [18]. FAM20B was identified as a kinase responsible for the 2-*O*-phosphorylation of xylose and shown to modulate the number of GAG chains [19]. Moreover, during the preparation of this manuscript, Hashiguchi et al. demonstrated the sulfotransferase activity of HNK-1ST toward the GlcA of the GAG-linkage region with an *in vitro* enzymatic assay system using a peptide containing the tetrasaccharide [20]. However, the biological significance of the sulfate group on GlcA remains unclear.

In this study, we explored the involvement of HNK-1ST in the modification of the protein-linkage region and regulation of GAG assembly. Using a soluble form of recombinant TM, we found that HNK-1ST actually sulfated the linkage region and induced immunoreactivity with a HNK-1 mAb. HNK-1ST had the ability to suppress the GAG-bearing form of TM (β-TM) and anti-coagulant activity of TM. Moreover, CS chain polymerization reaction was not observed on the HNK-1-positive TM, suggesting the terminal 3-*O*-sulfation of the linkage tetrasaccharide to act as an inhibitory signal for the initiation of GAG biosynthesis.

2. Materials and methods

2.1. Materials

HNK-1 mAb was purchased from the American Type Culture Collection. The mouse anti-EGFP and anti-myc mAbs were from Clontech and Millipore, respectively. The HRP-conjugated anti-mouse IgG and anti-mouse IgM were obtained from Invitrogen. The nickel–nitrilotriacetic acid (Ni–NTA)-conjugated agarose was from Qiagen. Chondroitinase ABC and peptide *N*-glycosidase F were purchased from Seikagaku Corp., Tokyo, Japan and Roche Applied Science, respectively. UDP-[^{3}H]GalNAc (10 Ci/mmol) was from NEN Life Science Products. Unlabeled UDP-GlcA and UDP-GalNAc were obtained from Sigma (St. Louis, MO, USA).

2.2. cDNA construction

The cDNA fragment encoding TM was amplified from a human leukocyte cDNA library (Clontech) as a template with the primers CGGGATCCGGTAACATGCTTGGGGTCCTG containing a *Bam*HI site and CCAAGCTTCGAATGCACGAGCCCCACGG containing a *Hind*III site. The PCR fragments were subcloned into pcDNA3.1(−) myc/His (Invitrogen) (sTM-myc). The expression plasmid for EGFP-tagged rat HNK-1ST (ST-EGFP) was described previously [16]. The plasmid encoding the R189A mutant of HNK-1ST (R189A-EGFP) was constructed from ST-EGFP, using a QuikChange Lightning Site-Directed Mutagenesis Kit (Stratagene) with the primers CAAGTTTTTTATTGTGGCGGATCCCTTTGAAAGACTGATCTCTGC and GCAGAGATCAGTCTTTCAAAGGGATCCGCCACAATAAAAAACTTG.

2.3. Cell culture and transfection

CHO-K1 cells were maintained in α-minimum essential medium with 10% fetal bovine serum (FBS) in 5% CO_2 at 37 °C. The cells were grown overnight and transfected with cDNA using Lipofectamine 2000 (Invitrogen) according to the manufacturer's instructions. The culture medium was replaced with serum-free OPTI-MEM I (Invitrogen) 5 h after transfection, and the cells were cultured another 2 days.

2.4. Western blot analysis

Proteins solubilized in Laemmli sample buffer were separated by SDS–PAGE using 7% polyacrylamide gels and then transferred to nitrocellulose membranes. After blocking with 5% nonfat dry milk in phosphate-buffered saline containing 0.05% Tween 20, the membranes were incubated with primary antibodies, followed by HRP-conjugated secondary antibodies. Protein bands were detected with Super Signal West Pico chemiluminescence reagent (Thermo Scientific) using a LAS-3000 Luminoimage Analyzer (FUJIFILM).

2.5. Purification of recombinant sTM-myc

CHO-K1 cells plated on 175 cm^2 tissue culture flasks were transfected with sTM-myc with or without ST-EGFP using the Lipofectamine 2000 transfection reagent. After 5 h, the culture medium was replaced with serum-free ASF104 medium (Ajinomoto), and the cells were cultured for another 3 days. Then, the culture medium containing secreted proteins was applied to a HisTrap TM HP column (GE Healthcare). Unbound proteins were washed out with more than 10 column volumes of phosphate buffer (pH 7.4) containing 300 mM NaCl and 20 mM imidazole. Bound proteins were eluted with phosphate buffer (pH 7.4) containing 300 mM NaCl and 500 mM imidazole. Then, the eluted materials were dialyzed with 20 mM Tris–HCl buffer (pH 7.4) containing 100 mM NaCl.

2.6. Measurement of the anti-coagulant activity of TM

The anti-coagulant activity of TM was determined by its ability to inhibit thrombin clotting activity with fibrinogen (Sigma) as described [10,21]. Fibrinogen clotting was monitored visually. Thrombin (18 nM, Sigma) was incubated for 1 min at 37 °C with TM, chondroitinase ABC-treated TM, or TM + HNK-1ST at various molar ratios. Fibrinogen (2.0 mg/ml, final concentration) was then added and the clotting time was determined. The assays were performed in 0.02 M Tris–HCl buffer (pH 7.5) containing 0.1 M NaCl and 1 mg/ml bovine serum albumin.

2.7. CS polymerization assay

The ChSy-1 and ChPF expression plasmids (3.0 μg each) were co-transfected into COS-1 cells on 100-mm plates using FuGENE™ 6 (Roche Molecular Biochemicals, Tokyo, Japan) as described previously [22]. Two days after transfection, 1 ml of the culture medium was collected and incubated with 10 μl of IgG-Sepharose (Amersham Pharmacia Biotech) for 1 h at 4 °C. The beads recovered by centrifugation were washed with and resuspended in the assay buffer, and then tested for GalNAc transferase activity, as described [23]. Polymerization reactions using TM or TM + HNK-1ST as acceptors were co-incubated in reaction mixtures containing the following constituents in a total volume of 50 μl: 0.1 nmol TM or TM + HNK-1ST, 0.25 mM UDP-[^{3}H]GalNAc (5×10^5 dpm), 0.25 mM UDP-GlcA, 100 mM MES buffer, pH 6.5, 10 mM $MnCl_2$, and 10 μl of the resuspended beads. The mixtures were incubated at 37 °C overnight. Products of the polymerization reactions were isolated by gel filtration using a syringe column packed with Sephadex G-25 (superfine) [24]. The flow-through fractions were collected, and radioactivity was measured by liquid scintillation spectrophotometry.

3. Results and discussion

3.1. HNK-1ST suppresses CS modification of TM

To investigate the involvement of HNK-1ST in the modification of the protein-linkage region in TM, a soluble form of myc/His-tagged TM (sTM-myc) was transiently expressed in CHO-K1 cells with or without EGFP-tagged HNK-1ST (ST-EGFP). Although TM is an integral membrane protein, sTM-myc is designed to be secreted into the culture medium by truncating the transmembrane domain. The secreted sTM-myc was pulled down from the culture medium with nickel–nitrilotriacetic acid (Ni–NTA)-conjugated agarose beads, and subjected to Western blotting. When sTM-myc was expressed alone, both TM glycoforms, the CS chain-bearing form (β-TM) and non-bearing form (α-TM), were detected by anti-myc antibody (Fig. 1A). After digestion with chondroitinase ABC (CSase ABC), the upper smear (β-TM) disappeared and converged with the 100 kDa band (α-TM) (Fig. 1B), indicating that sTM-myc was actually modified by the CS chain in CHO-K1 cells. Interestingly, however, with the co-expression of sTM-myc and ST-EGFP, β-TM production was markedly reduced, and conversely, the amount of α-TM increased, indicating that most TM remains as a CS chain-lacking α-form in the presence of HNK-1ST (Fig. 1A). Moreover, HNK-1 immunoreactivity was detected on the α-form of sTM-myc co-expressed with ST-EGFP (Fig. 1A). Since neither GlcAT-P nor GlcAT-S is endogenously expressed in CHO-K1 cells, the HNK-1 epitope might be synthesized by GlcAT-I and HNK-1ST. To further characterize the HNK-1 epitope on sTM-myc, HNK-1-positive sTM-myc was treated with peptide *N*-glycosidase F (PNGase F) to remove the *N*-linked glycans. The molecular weight of sTM-myc was slightly decreased, but HNK-1 immunoreactivity was unchanged after the PNGase F treatment (Fig. 1C), indicating that TM carries *N*-linked glycans but the HNK-1 epitope does not attach to it. Considering our previous finding that the linkage tetrasaccharide (GlcAβ1-3Galβ1-3Galβ1-4Xyl) is the only oligosaccharide detected on α-TM expressed in CHO-K1 cells and HNK-1ST transfers a sulfate group to the C-3 position of the non-reducing terminal GlcA, HNK-1ST appeared to be involved in the biosynthesis of the GAG-linkage-type HNK-1 epitope (HSO_3-3GlcAβ1-3Galβ1-3Galβ1-4Xyl) found in human urine [17].

3.2. The sulfotransferase activity of HNK-1ST is required for regulating the attachment of the CS chain

Next, to determine the requirement of the enzymatic activity of HNK-1ST to arrest the initiation of the CS chain, we generated an activity-depleted mutant of HNK-1ST, which harbors a mutation of Arg^{189} to Ala (R189A-EGFP). This mutant is reported to show almost no activity due to impaired binding to the donor substrate, 3′-phosphoadenosine 5′-phosphosulfate (PAPS) [25]. When co-expressed with R189A-EGFP, sTM-myc contained a comparable amount of the β-form to that expressed alone and did not exhibit HNK-1 immunoreactivity on its α-form (Fig. 2). This result indicates that the regulatory function of HNK-1ST is achieved by the transfer of a sulfate group to the C-3 position of GlcA. Taken together, these results suggest that the sulfation of terminal GlcA in the GAG-linkage tetrasaccharide by HNK-1ST negatively regulates the CS chain on TM.

3.3. HNK-1ST controls the anti-coagulant activity of TM by regulating the attachment of the CS chain

TM is expressed on the endothelial cell surface, and plays a pivotal role in anti-coagulation, including the inhibition of the procoagulant activity of thrombin [10]. Since the anti-coagulant activity of TM is highly dependent on its CS chain [10,12], we examined whether HNK-1ST is able to control the function of TM by regulating the attachment of the CS chain. To measure anti-coagulant activity, we purified the recombinant sTM-myc from the culture medium of CHO-K1 cells with or without ST-EGFP co-expression.

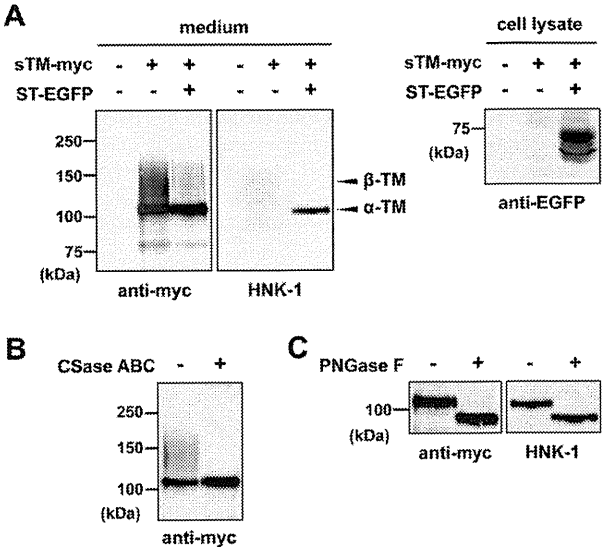

Fig. 1. Effect of HNK-1ST on the expression of the HNK-1 epitope and CS chain on TM. (A) sTM-myc with or without HNK-1ST-EGFP (ST-EGFP) was transiently expressed in CHO-K1 cells. The secreted sTM-myc was pulled down from the culture medium and subjected to Western blotting using anti-myc and HNK-1 mAb (*medium*). The two glycoforms of TM (α- and β-TM) were detected (*arrowheads*). The CHO-K1 cell lysate was analyzed for HNK-1ST-EGFP expression (*cell lysate*). (B) sTM-myc was treated with chondroitinase ABC (CSase ABC) to remove the CS moiety and Western blotted with anti-myc mAb. (C) sTM-myc was prepared from HNK-1ST-EGFP co-expressing cells and treated with peptide *N*-glycosidase F (PNGase F), and subjected to Western blotting with anti-myc and HNK-1 mAb.

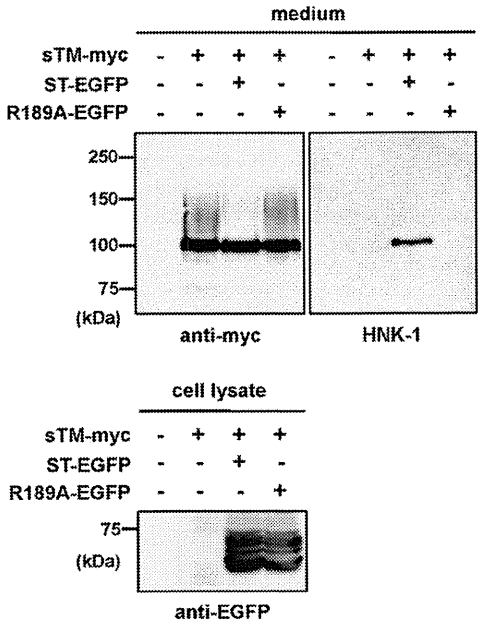

Fig. 2. Requirement of the sulfotransferase activity of HNK-1ST for the suppression of CS chain on TM. sTM-myc was co-transfected with ST-EGFP or the R189A mutant of HNK-1ST (R189A-EGFP). The secreted sTM-myc was pulled down and subjected to Western blotting using anti-myc and HNK-1 mAb (*medium*). The expression of HNK-1ST and HNK-1ST (R189A) was confirmed by Western blotting of the cell lysate (*cell lysate*).

The purity of the recombinant protein was confirmed by CBB staining and Western blotting (Fig. 3A and B). Consistent with the data shown in Fig. 1, co-expression of HNK-1ST resulted in a reduction in β-TM and the appearance of HNK-1-immunoreactivity (Fig. 3A and B). Then, a thrombin-dependent clotting assay was performed to evaluate the anti-coagulant activity of purified sTM-myc. sTM-myc (TM in Fig. 3C), which was not co-expressed with ST-EGFP, caused a dose-dependent delay in the clotting time, while the removal of the CS chain by the pre-treatment with CSase ABC greatly abrogated the anti-coagulant activity of sTM-myc (TM(CSase) in Fig. 3C). Then, we employed the same assay using sTM-myc co-expressed with ST-EGFP (TM + HNK-1ST). TM + HNK-1ST showed almost no inhibition of thrombin-induced clotting, similar to the CSase-treated sTM-myc (Fig. 3C). These results suggest that TM is scarcely modified by the CS chain in the presence of HNK-1ST, leading to the loss of TM function.

3.4. The terminal 3-O-sulfation of the linkage tetrasaccharide has an inhibitory function in the initiation of CS biosynthesis

The initiation and elongation of CS chains are conducted by an enzyme complex of chondroitin synthase (ChSy-1 to 3) and chondroitin polymerizing factor (ChPF) [22,26]. Therefore, to demonstrate that the terminal sulfate group transferred by HNK-1ST to the linkage tetrasaccharide indeed acts as a stop signal that inhibits the addition of CS, we measured the chondroitin-polymerizating activity of ChSy/ChPF against sTM-myc described in Fig. 3. When sTM-myc expressed without ST-EGFP (TM in Table 1) was used as an acceptor substrate, significant polymerization by ChSy/ChPF (17.8 pmol/mg/h) was observed (Table 1). However, we could not detect any activity against sTM-myc co-expressed with ST-EGFP (TM + HNK-1ST in Table 1), indicating that the sulfated linkage region tetrasaccharide is not utilized as a substrate for CS-polymerizing enzymes.

In this report, we demonstrated that HNK-1ST synthesizes a HNK-1 antibody-reactive epitope on α-TM and suppresses the expression of β-TM in an activity-dependent manner. We also produced evidence that α-TM bearing this epitope is not utilized as a substrate for CS-polymerizing enzymes. We did not precisely determine the structure of the HNK-1-reactive epitope but the sulfate group transferred by HNK-1ST is presumably expressed on the terminal GlcA at the C-3 position of the GAG-linkage region. The reason for this is that HNK-1ST is known to transfer a sulfate group from PAPS to the C-3 position of the non-reducing terminal GlcA residue and the resultant epitope is recognized by HNK-1 antibody

Table 1
Chondroitin polymerization on HNK-1-positive sTM-myc.

Acceptor substrate	Polymerization activity
	pmol/mg/h
TM (0.1 nmol)	17.8
TM + HNK-1ST (0.1 nmol)	ND[a]

[a] ND, not detected (<0.01 pmol/mg/h).

[27]. Furthermore, Hashiguchi et al. have directly demonstrated the sulfotransferase activity of HNK-1ST toward the GlcA of the GAG-linkage region with an *in vitro* enzymatic assay system using chemically synthesized substrates. These results suggest that HNK-1ST forms an enzyme complex with GlcAT-I and regulates the expression of the CS chain of TM to control anti-coagulation.

Since 3-*O*-sulfation suppressed the assembly of CS, this sulfate group might be used as an inhibitory signal to control the function of PGs through the modification of GAGs. At the initiation step of the polymerization of CS chains, the first GalNAc is transferred to the C-4 position of the terminal GlcA of the linkage region tetrasaccharide [1]. Therefore, the 3-*O*-sulfation by HNK-1ST does not directly compete with the transfer of the first GalNAc, and there might be an underlying mechanism by which the sulfate group inhibits the initial GalNAc-transfer, for example, steric hindrance. Although we have shown the effect of 3-*O*-sulfation on the attachment of CS chains, its influence on HS synthesis is unclear. Since the first GlcNAc of HS chains is also transferred to the C-4 position of the terminal GlcA, it is possible that the 3-*O*-sulfate exerts a similar inhibitory effect on the assembly of HS. However, the linkage tetrasaccharide containing 3-*O*-sulfated GlcA on HS-bearing PGs is still to be identified.

HNK-1ST is generally known as a sulfotransferase involved in the biosynthesis of a HNK-1 carbohydrate epitope mainly expressed on *N*-glycans in the nervous system. The expression of the HNK-1 carbohydrate is predominantly restricted to the nervous tissue due to limited distributions of GlcAT-P and GlcAT-S [28,29]. HNK-1ST, however, is more ubiquitous than GlcAT-P or GlcAT-S [27,30], supporting our idea that HNK-1ST contributes to the regulation of GAG attachment, a second role different from that in the biosynthesis of the HNK-1 epitope expressed on *N*-glycans.

The 3-*O*-sulfated tetrasaccharide structure has been found in α-TM purified from human urine and serum [17,20]. In this study, we demonstrated that the sulfated structure is biosynthesized by HNK-1ST and is not utilized as a substrate for CS-polymerizing enzymes. These lines of evidence indicate the possibility that the

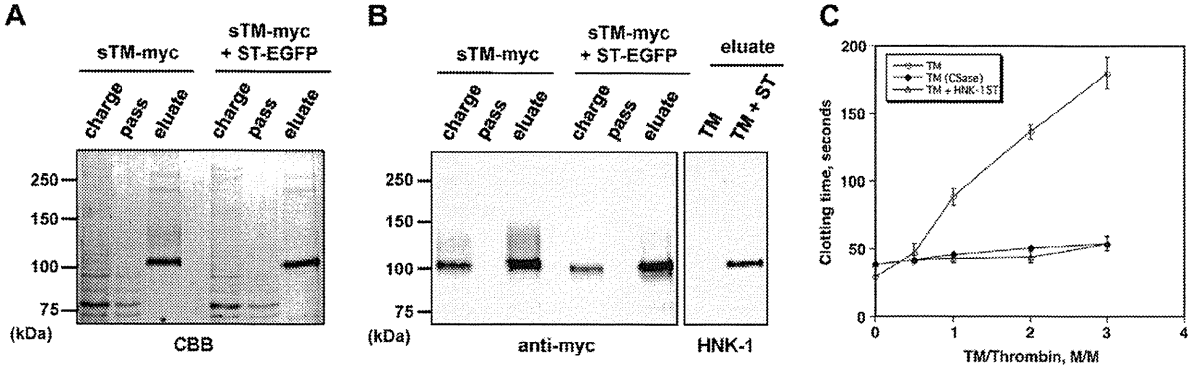

Fig. 3. The effect of HNK-1ST on the anti-coagulant activity of TM. (A and B) sTM-myc expressed in the absence or presence of ST-EGFP was purified from the culture medium of CHO-K1 cells using a HisTrap column. The culture medium (*charge*), the pass-through fraction (*pass*), and the eluate were analyzed by CBB staining (A) and Western blotting using anti-myc (B). The HNK-1 expression was also assessed using the eluates (B). (C) The purified sTM-myc was subjected to the thrombin-dependent clotting assay. sTM-myc (TM, *open circle*), sTM-myc pre-treated with CSase ABC (TM(CSase), *filled circle*), and sTM-myc co-expressed with HNK-1ST (TM + HNK-1ST, *triangle*) were mixed with thrombin at different molar ratios as indicated and clotting time was measured.

CS-modulating function of HNK-1ST is employed to maintain the homeostasis of the blood circulation system *in vivo*. In CHO-K1 cells, however, a significant amount of α-TM bearing un-sulfated tetrasaccharide linkage structure was expressed even without HNK-1ST transfection (Fig. 1B, and [11]), indicating the presence of another regulatory mechanism of part-time PGs. Since the CS of TM plays a crucial role in its anti-coagulant activities, it is of great interest to clarify the overall sorting mechanism for part-time PGs.

Acknowledgments

This work was supported in part by Grant-in-Aid for Scientific Research (B) 21370053 (to S. O.) from JSPS and for Scientific Research on Innovative Areas (to S.O. and H.K.) from MEXT, and in part by Health and Labour Sciences Research Grant on Comprehensive Research on Disability Health and Welfare, H21-012 (to S.O. and H.K.).

References

[1] K. Sugahara, H. Kitagawa, Recent advances in the study of the biosynthesis and functions of sulfated glycosaminoglycans, Curr. Opin. Struct. Biol. 10 (2000) 518–527.
[2] C. Götting, J. Kuhn, R. Zahn, T. Brinkmann, K. Kleesiek, Molecular cloning and expression of human UDP-D-Xylose: proteoglycan core protein β-D-Xylosyltransferase and its first isoform XT-II, J. Mol. Biol. 304 (2000) 517–528.
[3] T. Okajima, K. Yoshida, T. Kondo, K. Furukawa, Human homolog of *Caenorhabditis elegans sqv*-3 gene is galactosyltransferase I involved in the biosynthesis of the glycosaminoglycan-protein linkage region of proteoglycans, J. Biol. Chem. 274 (1999) 22915–22918.
[4] R. Almeida, S.B. Levery, U. Mandel, H. Kresse, T. Schwientek, E.P. Bennett, H. Clausen, Cloning and expression of a proteoglycan UDP-galactose: β-xylose β1,4-galactosyl-transferase I. A seventh member of the human β4-galactosyltransferase gene family, J. Biol. Chem. 274 (1999) 26165–26171.
[5] X. Bai, D. Zhou, J.R. Brown, B.E. Crawford, T. Hennet, J.D. Esko, Biosynthesis of the linkage region of glycosaminoglycans: cloning and activity of galactosyltransferase II, the sixth member of the beta 1,3-galactosyltransferase family (beta 3GalT6), J. Biol. Chem. 276 (2001) 48189–48195.
[6] H. Kitagawa, Y. Tone, J. Tamura, K.W. Neumann, T. Ogawa, S. Oka, T. Kawasaki, K. Sugahara, Molecular cloning and expression of glucuronyltransferase I involved in the biosynthesis of the glycosaminoglycan-protein linkage region of proteoglycans, J. Biol. Chem. 273 (1998) 6615–6618.
[7] K. Sugahara, T. Mikami, T. Uyama, S. Mizuguchi, K. Nomura, H. Kitagawa, Recent advances in the structural biology of chondroitin sulfate and dermatan sulfate, Curr. Opin. Struct. Biol. 13 (2003) 612–620.
[8] N. Perrimon, M. Bernfield, Specificities of heparan sulphate proteoglycans in developmental processes, Nature 404 (2000) 725–728.
[9] L.Å. Fransson, Structure and function of cell-associated proteoglycans, Trends Biochem. Sci. 12 (1987) 406–411.
[10] K.T. Preissner, T. Koyama, D. Müller, J. Tschopp, G. Müller-Berghaus, Domain structure of the endothelial cell receptor thrombomodulin as deduced from modulation of its anticoagulant functions. Evidence for a glycosaminoglycan-dependent secondary binding site for thrombin, J. Biol. Chem. 265 (1990) 4915–4922.
[11] S. Nadanaka, H. Kitagawa, K. Sugahara, Demonstration of the immature glycosaminoglycan tetrasaccharide sequence GlcAβ1-3Galβ1-3Galβ1-4Xyl on recombinant soluble human α-thrombomodulin. A possible mechanism generating 'part-time' proteoglycan, J. Biol. Chem. 273 (1998) 33728–33734.
[12] K. Nawa, K. Sakano, H. Fujiwara, Y. Sato, N. Sugiyama, T. Teruuchi, M. Iwamoto, Y. Marumoto, Presence and function of chondroitin-4-sulfate on recombinant human soluble thrombomodulin, J. Biol. Chem. 171 (1990) 729–737.
[13] S. Yamamoto, S. Oka, M. Inoue, M. Shimuta, T. Manabe, H. Takahashi, M. Miyamoto, M. Asano, J. Sakagami, K. Sudo, Y. Iwakura, K. Ono, T. Kawasaki, Mice deficient in nervous system-specific carbohydrate epitope HNK-1 exhibit impaired synaptic plasticity and spatial learning, J. Biol. Chem. 277 (2002) 27227–27231.
[14] I. Morita, S. Kakuda, Y. Takeuchi, T. Kawasaki, S. Oka, HNK-1 (human natural killer-1) glyco-epitope is essential for normal spine morphogenesis in developing hippocampal neurons, Neuroscience 164 (2009) 1685–1694.
[15] I. Morita, S. Kakuda, Y. Takeuchi, S. Itoh, N. Kawasaki, Y. Kizuka, T. Kawasaki, S. Oka, HNK-1 glyco-epitope regulates the stability of the glutamate receptor subunit GluR2 on the neuronal cell surface, J. Biol. Chem. 284 (2009) 30209–30217.
[16] Y. Kizuka, T. Matsui, H. Takematsu, Y. Kozutsumi, T. Kawasaki, S. Oka, Physical and functional association of glucuronyltransferases and sulfotransferase involved in HNK-1 biosynthesis, J. Biol. Chem. 281 (2006) 13644–13651.
[17] H. Wakabayashi, S. Natsuka, T. Mega, N. Otsuki, M. Isaji, M. Naotsuka, S. Koyama, T. Kanamori, K. Sakai, S. Hase, Novel proteoglycan linkage tetrasaccharides of human urinary soluble thrombomodulin, SO_4-3GlcAβ1-3Galβ1-3(+/-Siaα2-6)Galβ1-4Xyl, J. Biol. Chem. 274 (1999) 5436–5442.
[18] Y. Tone, L.C. Pedersen, T. Yamamoto, T. Izumikawa, H. Kitagawa, J. Nishihara, J. Tamura, M. Negishi, K. Sugahara, 2-*O*-phosphorylation of xylose and 6-*O*-sulfation of galactose in the protein linkage region of glycosaminoglycans influence the glucuronyltransferase-I activity involved in the linkage region synthesis, J. Biol. Chem. 283 (2008) 16801–16807.
[19] T. Koike, T. Izumikawa, J. Tamura, H. Kitagawa, FAM20B is a kinase that phosphorylates xylose in the glycosaminoglycan-protein linkage region, Biochem. J. 421 (2009) 157–162.
[20] T. Hashiguchi, S. Mizumoto, Y. Nishimura, J.I. Tamura, S. Yamada, K. Sugahara, Involvement of HNK-1 sulfotransferase in the biosynthesis of the GlcUA(3-*O*-sulfate)-Gal-Gal-Xyl tetrasaccharide found in α-thrombomodulin from human urine, J. Biol. Chem. 286 (2011) 33003–33011.
[21] C.T. Esmon, N.L. Esmon, K.W. Harris, Complex formation between thrombin and thrombomodulin inhibits both thrombin-catalyzed fibrin formation and factor V activation, J. Biol. Chem. 257 (1982) 7944–7947.
[22] H. Kitagawa, T. Izumikawa, T. Uyama, K. Sugahara, Molecular cloning of a chondroitin polymerizing factor that cooperates with chondroitin synthase for chondroitin polymerization, J. Biol. Chem. 278 (2003) 23666–23671.
[23] H. Kitagawa, K. Tsutsumi, M. Ujikawa, F. Goto, J. Tamura, K. Neumann, T. Ogawa, K. Sugahara, Regulation of chondroitin sulfate biosynthesis by specific sulfation: acceptor specificity of serum β-GalNAc transferase revealed by structurally defined oligosaccharides, Glycobiology 7 (1997) 531–537.
[24] H. Kitagawa, K. Tsuchida, M. Ujikawa, K. Sugahara, Detection and characterization of UDP-GalNAc: chondroitin *N*-acetylgalactosaminyltransferase in bovine serum using a simple assay method, J. Biochem. 117 (1995) 1083–1087.
[25] E. Ong, J.C. Yeh, Y. Ding, O. Hindsgaul, L.C. Pedersen, M. Negishi, M. Fukuda, Structure and function of HNK-1 sulfotransferase. Identification of donor and acceptor binding sites by site-directed mutagenesis, J. Biol. Chem. 274 (1999) 25608–25612.
[26] T. Izumikawa, T. Koike, S. Shiozawa, K. Sugahara, J. Tamura, H. Kitagawa, Identification of chondroitin sulfate glucuronyltransferase as chondroitin synthase-3 involved in chondroitin polymerization: chondroitin polymerization is achieved by multiple enzyme complexes consisting of chondroitin synthase family members, J. Biol. Chem. 283 (2008) 11396–11406.
[27] E. Ong, J.C. Yeh, Y. Ding, O. Hindsgaul, M. Fukuda, Expression cloning of a human sulfotransferase that directs the synthesis of the HNK-1 glycan on the neural cell adhesion molecule and glycolipids, J. Biol. Chem. 273 (1998) 5190–5195.
[28] K. Terayama, S. Oka, T. Seiki, Y. Miki, A. Nakamura, Y. Kozutsumi, K. Takio, T. Kawasaki, Cloning and functional expression of a novel glucuronyltransferase involved in the biosynthesis of the carbohydrate epitope HNK-1, Proc. Natl. Acad. Sci. USA 94 (1997) 6093–6098.
[29] T. Seiki, S. Oka, K. Terayama, K. Imiya, T. Kawasaki, Molecular cloning and expression of a second glucuronyltransferase involved in the biosynthesis of the HNK-1 carbohydrate epitope, Biochem. Biophys. Res. Commun. 255 (1999) 182–187.
[30] H. Tagawa, Y. Kizuka, T. Ikeda, S. Itoh, N. Kawasaki, H. Kurihara, M.L. Onozato, A. Tojo, T. Sakai, T. Kawasaki, S. Oka, A non-sulfated form of the HNK-1 carbohydrate is expressed in mouse kidney, J. Biol. Chem. 280 (2005) 23876–23883.

Glycobiology vol. 22 no. 1 pp. 84–95, 2012
doi:10.1093/glycob/cwr107
Advance Access publication on August 10, 2011

Role of interaction of mannan-binding protein with meprins at the initial step of complement activation in ischemia/reperfusion injury to mouse kidney

Makoto Hirano[2,3,4,8], Bruce Y Ma[3,5,6,9], Nobuko Kawasaki[3], Shogo Oka[7], and Toshisuke Kawasaki[1,3]

[2]Department of Biological Chemistry, Graduate School of Pharmaceutical Sciences, Kyoto University, Kyoto 606-8501, Japan; [3]Research Center for Glycobiotechnology, Ritsumeikan University, Shiga 525-0058, Japan; [4]Institute of Glycoscience, Tokai University, Kanagawa 259-1292, Japan; [5]Department of Computer Science and Systems Engineering, Muroran Institute of Technology, Hokkaido 050-8585, Japan; [6]School of Pharmaceutical Engineering and Life Science, Changzhou University, Jiangsu 213164, People's Republic of China; and [7]School of Health Sciences, Faculty of Medicine, Kyoto University, Kyoto 606-8501, Japan

Received on May 13, 2011; revised on July 20, 2011; accepted on July 29, 2011

Ischemia/reperfusion (I/R) is an important cause of acute renal failure. Recent studies have shown that the complement system mediated by the mannan-binding protein (MBP), which is a C-type serum lectin recognizing mannose, fucose and *N*-acetylglucosamine residues, plays a critical role in the pathogenesis of ischemic acute renal failure. MBP causes complement activation through the MBP lectin pathway and a resulting complement component, C3b, is accumulated on the brush borders of kidney proximal tubules in a renal I/R-operated mouse kidney. However, the initial step of the complement activation has not been studied extensively. We previously identified both meprins α and β, highly glycosylated zinc metalloproteases, localized on kidney proximal tubules as endogenous MBP ligands. In the present study, we demonstrated that serum-type MBP (S-MBP) and C3b were co-localized with meprins on both the cortex and the medulla in the renal I/R-operated mouse kidney. S-MBP was indicated to interact with meprins in vivo in the I/R-operated mouse kidney and was shown to initiate the complement activation through the interaction with meprins in vitro. Taken together, the present study strongly suggested that the binding of S-MBP to meprins triggers the complement activation through the lectin pathway and may cause the acute renal failure due to I/R on kidney transplantation and hemorrhagic shock.

Keywords: cute renal failure / C3b / complement activation / C-type lectin / lectin pathway

Introduction

Ischemia/reperfusion (I/R) is an important cause of acute renal failure. Various clinical conditions such as intravascular volume depletion and hypotension can result in a reduction in renal blood flow, which leads to ischemic acute renal failure (Thadhani et al. 1996). The pathophysiology of renal I/R injury is complicated, but recent studies indicated that activation of complement through the lectin pathway plays a critical role in the pathogenesis of ischemic acute renal failure (de Vries et al. 2004). In the lectin pathway, mannan-binding protein (MBP), also known as mannan-binding lectin (MBL), binds to ligand carbohydrates on the cell surface and activates MBP-associated serine proteases (MASPs). Subsequently, activated MASPs cleave complement components C2 and C4 to yield C3 convertase, which can lead MBP-bound cells to necrosis. However, it is not clear what molecules interact with MBP at the initial stage of the complement activation in renal I/R. Although immunoglobulin M (IgM) triggers the lectin pathway in mesenteric I/R (Zhang et al. 2006), renal I/R does not induce IgM deposition (Park et al. 2002).

MBP recognizes D-mannose, L-fucose and *N*-acetyl-D-glucosamine residues Ca^{2+}-dependently. Human have only one MBP gene, whereas rodents have two MBPs encoded by separate genes, one is serum-type MBP termed S-MBP, MBL-1 or MBL-A and the other is liver-type MBP termed L-MBP, MBL-2 or MBL-C. Both MBPs are mostly synthesized by hepatocytes and secreted into the serum. However, a small amount of S-MBP, but not L-MBP, is synthesized in the mouse (Wagner et al. 2003) and rat (Morio et al. 1997) kidneys. Both mouse S- and L-MBPs can mediate the activation of C4 (Hansen et al. 2000; Liu et al. 2001), although they recognize different bacterial pathogens (Phaneuf et al. 2007).

We previously reported that endogenous MBP ligands are highly expressed on the brush borders of proximal tubules of the normal mouse kidney and the ligands were identified as

[1]To whom correspondence should be addressed: Tel: +81-77-561-3444; Fax: +81-77-561-3444; e-mail: tkawasak@fc.ritsumei.ac.jp
[8]Present address: Institute of Glycoscience, Tokai University, Kanagawa 259-1292, Japan.
[9]Present address: School of Pharmaceutical Engineering and Life Science, Changzhou University, Jiangsu 213164, People's Republic of China.

meprins α and β (Hirano et al. 2005). Meprins are highly glycosylated zinc metalloproteases abundantly expressed in kidney and intestinal epithelial cells, comprising ~5% of the total brush border membrane proteins in the rodent kidneys (Bond and Beynon 1986). Mouse meprin A (EC 3.4.24.18) is a homo-oligomer of α subunits or a hetero-oligomer of α and β subunits (Marchand et al. 1994). Mouse meprin B (EC 3.4.24.63) is a homo-oligomer of β subunits (Gorbea et al. 1993). Meprin α and β subunits form a disulfide-linked dimer and higher-order oligomers through non-covalent interactions (Gorbea et al. 1991). Meprin α has a tendency to form huge complexes with a molecular mass of 1–8 MDa, which comprise 10–100 subunits (Ishmael et al. 2001).

In the present study, we studied the functional role of interaction of MBP with meprins in the I/R-operated mouse kidney, because of the facts that meprins are endogenous ligands for MBP, abundantly expressed in the kidneys and self-aggregate into high-molecular mass complexes that is an important requirement for complement activation to occur. We demonstrated that recombinant mouse S-MBP, but not L-MBP, significantly activated complement by binding to meprins in vitro. Immunohistochemical analysis indicated that S-MBP partially co-localized with meprins in vivo. Additionally, the results of immunoprecipitation (IP) of meprins or S-MBP and in situ proximity ligation assay (PLA; Söderberg et al. 2006) of the renal I/R-operated mouse kidney indicated strongly the functional interaction of S-MBP with meprins in vivo. Protein quantification by western blotting indicated that the amount of S-MBP increased several-fold in the I/R-operated mouse kidney, whereas real-time polymerase chain reaction (PCR) revealed that the amount of S-MBP messenger RNA (mRNA) did not increase in the I/R-operated kidney. These results suggested the possibility that S-MBP increment in the I/R-operated kidney may be due to outflow from the blood circulation rather than the induction of S-MBP mRNA expression in the kidney. Thus, our findings suggested that S-MBP mostly derived from serum interact with meprins and initiates the complement activation through the lectin pathway in renal I/R injury.

Results

Preparation of I/R-operated mice

The experimental renal I/R-operated mouse has been established as a model of acute renal failure. Mice subjected to renal I/R operation exhibited the renal deposition of MBP and complement components and induction of tubular necrosis through the formation of membrane attack complexes (de Vries et al. 2004). We found a high-level expression of endogenous ligands for MBP in the epithelial cells of the kidney proximal tubules and subsequently identified metalloproteases, meprins α and β (meprins) as the predominant MBP ligands (Hirano et al. 2005). Based on this background, we hypothesized that the interaction of MBP with meprins may trigger the activation of complement, resulting in tubular necrosis. In order to test this, we investigated the localization of MBP, meprins and complement component C3b, an activated form of C3, and the protein levels of MBP and meprins, and also the mRNA expression levels of these proteins in the renal I/R-operated mouse kidney. Ischemia was induced by bilateral renal artery clamping and blood urea nitrogen (BUN) was monitored as an index of renal injury. Table I shows BUN level time courses in sham- and I/R-operated mice ($n = 4$). The starting point (0 h) indicates the time when the clamps were removed from the renal arteries. BUN increased gradually during reperfusion and reached at ~3- and 6-fold higher values after 6 and 24 h reperfusion in I/R-operated mice, respectively. We used I/R-operated mice that had reperfused for 6 h in the following experiments.

The localization of meprins, S-MBP and complement C3b in the I/R-operated mouse kidney

Immunohistochemical analysis using a laser confocal microscope indicated marked changes in the distribution of meprin β, S-MBP and C3b in association with I/R operation (Figures 1 and 2). Thus, meprin β was strictly localized in the cortex in the sham-operated mouse kidney (Figure 1A), whereas in the I/R-operated kidney, meprin β was expressed not only in the cortex but also in the medulla significantly (Figure 1G). To the contrary, S-MBP was not detected in the sham-operated kidney (Figure 1B). In the clear contrast to this, in the I/R-operated mouse kidney, S-MBP was massively accumulated in the cortex and, in addition, weak staining was detected in some parts of the medulla (Figure 1H). In higher-magnification views, meprin β in the cortex of the sham-operated mouse kidney was selectively localized on the apical surface of the proximal tubules (Figure 1E). On the other hand, in the I/R-operated mouse kidney, a significant portion of meprin β was detected on the base of the brush border, although there were slight morphological changes in the I/R-operated mouse kidney (Figure 1K). Overlay images indicated that S-MBP was co-localized with meprin β on the base of the brush border of the proximal tubules (Figure 1K) and the medulla (Figure 1L).

Figure 2 indicates that similar changes occurred in the distribution of a complement component, C3b, in association with I/R operation. C3b was hardly detected in the sham-operated mouse kidney (Figure 2B). In the clear contrast, in the I/R-operated mouse kidney, C3b was heavily

Table I. Determination of BUN (mg/dL) before and after renal I/R operation

Time (h)	−0.67	0	1	3	6	12	24
Sham	24 ± 4.3	24 ± 4.1	27 ± 4.4	25 ± 2.8	28 ± 3.0	24 ± 8.0	20 ± 2.8
I/R	25 ± 3.0	32 ± 3.0	38 ± 3.9	56 ± 7.8	73 ± 14.5	124 ± 22.7	160 ± 45.0

Renal function before ischemia (−0.67) and 0, 1, 3, 6, 12 and 24 h after 40 min ischemia. The data are expressed as mean ± SD ($n = 4$).

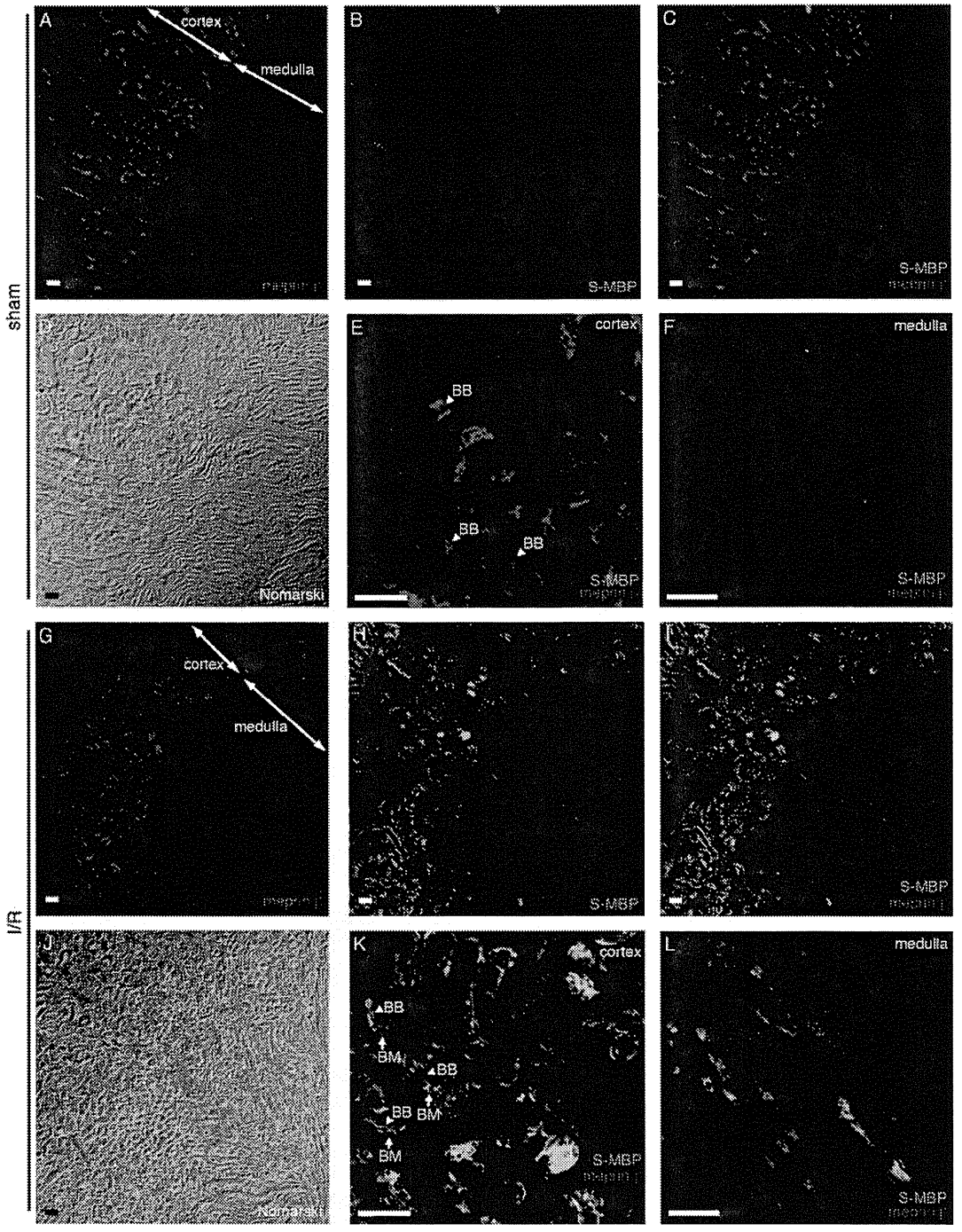

Fig. 1. Localization of S-MBP and meprin β in the renal I/R-operated mouse kidney. Representative kidney paraffin sections (10 μm) were harvested following renal I/R (reperfused for 6 h) and stained with both anti-meprin β and anti-S-MBP antibodies. Cortical and medullary regions are indicated with double arrows in (A) and (G). (**A**) Meprin β (red) was localized strictly in the cortex. (**G**) Meprin β was localized not only in the cortex but also in the medulla. (**B**) S-MBP (green) was not detected. (**H**) S-MBP massively deposited in the cortex and, in addition, S-MBP was weakly detected in the medulla. (**C**) Overlay image of (A) with (B). (**I**) Overlay image of (G) with (H) shows that S-MBP is co-localized with meprin β mostly in the cortex. (**D** and **J**) Nomarski microphotographs of (A)–(C) and (G) and (H), respectively. (**E**, **K**, **F** and **L**) Higher-magnification views of cortical regions of (C) and (I) and medullary regions of (C) and (I), respectively. Arrowheads and arrows indicate the brush border membranes (BB) and the basolateral membranes (BM) of the proximal tubules, respectively. (**E**) Meprin β was strictly localized on the brush border membrane of the proximal tubules, but S-MBP was not detected. (**K**) The brush border membranes of the proximal tubules changed morphologically. S-MBP was partially co-localized with meprin β on the base of the brush border membrane of the proximal tubules. (**F**) Neither S-MBP nor meprin β were detected. (**L**) S-MBP was partially co-localized with meprin β. Bars, 100 μm.

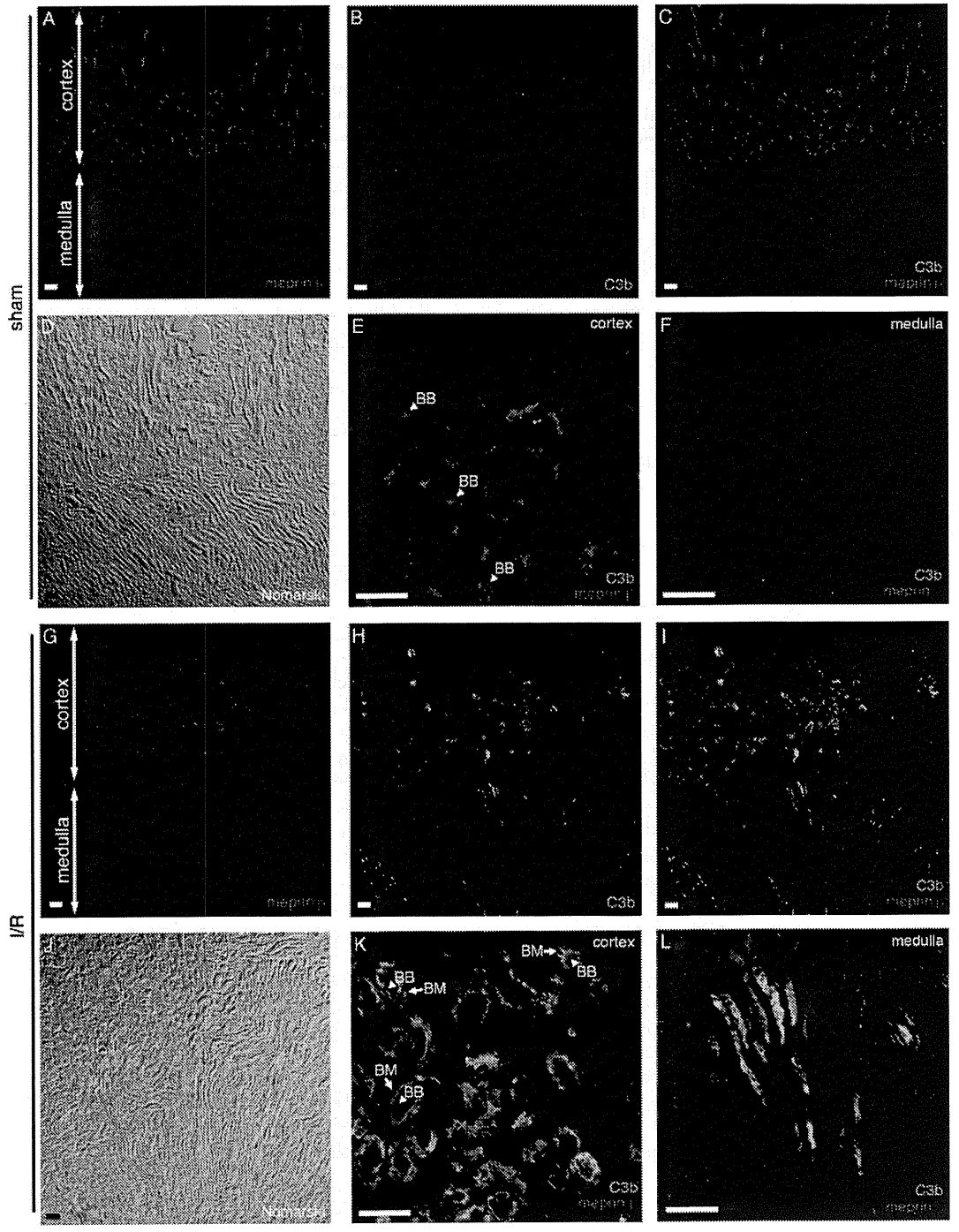

Fig. 2. Localization of C3b and meprin β in the renal I/R-operated mouse kidney. Representative kidney paraffin sections (10 μm) were harvested following renal I/R (reperfused for 6 h) and stained with both anti-meprin β and anti-C3b antibodies. Cortical and medullary regions are indicated with double arrows in (A) and (G). (**A**) Anti-meprin β (red) strictly stained the cortex. (**G**) Anti-meprin β stained not only the cortex but also the medulla. (**B**) C3b (green) was not detected. (**H**) C3b was detected abundantly in the cortex and weakly in the medulla. (**C**) Overlay image of (A) with (B). (**I**) Overlay image of (G) with (H) shows that C3b is co-localized with meprin β mostly in the cortex. (**D** and **J**) Nomarski microphotographs of (A)–(C) and (G) and (H), respectively. (**E**, **K**, **F** and **L**) Higher-magnification views of cortical regions of (C) and (I) and medullary regions of (C) and (I), respectively. Arrowheads and arrows indicate the brush border membranes (BB) and the basolateral membranes (BM) of the proximal tubules, respectively. (**E**) Meprin β was strictly localized on the brush border membrane of the proximal tubules. No signals of C3b were detected. (**K**) C3b was co-localized with meprin β mostly on the base of the brush border membrane of the proximal tubules. (**F**) Neither C3b nor meprin β were detected. (**L**) C3b was partially co-localized with meprin β. Bars, 100 μm.

accumulated in the proximal tubular cells (Figure 2H). C3b was co-localized with meprin β for the most part on the brush border membranes of the proximal tubules (Figure 2K) and in the medulla (Figure 2L).

The immunohistochemical data presented in Figures 1 and 2 indicate clearly that meprin β is an intrinsic component of the normal brush border membranes of the proximal tubules in the cortex, while S-MBP and C3b are not the normal components in this part of the mouse kidney and they appeared only after I/R operation. In addition, the strict localization of meprin β in the cortex was partially abolished and meprin β appeared in the medulla to some extent. Interestingly, S-MBP and C3b, which appeared in the kidney after I/R operation, are co-localized with meprin β on the base of the brush border of the proximal tubules, suggesting a possibility of a functional contact between meprin β and S-MBP. Furthermore, meprin α was co-localized with both S-MBP and C3b in the same manner as meprin β, and L-MBP could not be detected in the kidney (data not shown).

In situ interaction of S-MBP with meprins in the I/R-operated mouse kidney

In order to examine the molecular interaction of S-MBP with meprins in vivo, co-IP experiments were carried out. Small pieces of sham- and I/R-operated mouse kidney cortexes ($n = 3$) were subjected to chemical cross-linking with dithiobis (succinimidylpropionate) (DSP), followed by homogenization and extraction with Nonidet P-40 (NP-40). NP-40 extracts were incubated with antibody specific to S-MBP or meprins, and the immunoprecipitates were analyzed by western blotting after sodium dodecyl sulfate (SDS)–polyacrylamide gel electrophoresis (PAGE). As shown in Figure 3A, multiple S-MBP bands, which probably represent monomer, dimer and trimer of the structural unit of S-MBP, were detected in co-immunoprecipitates with either meprin α (left panel) or meprin β (right panel) as indicated by arrowheads. The estimated molecular masses of trimer, dimer and monomer of the structural unit of S-MBP were 220, 160 and 117 kDa, respectively; in contrast, theoretical molecular masses of trimer, dimer and monomer of the structural unit were ~270, 180 and 90 kDa, respectively. Thus, higher oligomers are estimated to be smaller than their respective theoretical values under non-reducing conditions tested. The reasons for these discrepancies are not clear at the moment but this might be due to incomplete denaturation of higher oligomers because of the presence of intrachain disulfide bonds within the monomeric subunit of S-MBP, interchain disulfide bonds between the subunit components of S-MBP and also newly formed cross-links by DSP treatment. Reversely, as shown in Figure 3B, multiple bands of meprins α and β, probably representing, homo- or heterodimers and trimers of meprins α (left panel) and β (right panel), respectively, were detected in co-immunoprecipitates with S-MBP as indicated by arrowheads. In these two sets of experiments, protein levels of S-MBP and meprins co-immunoprecipitated with meprins and S-MBP, respectively, from the I/R-operated mouse kidney were significantly higher than those from the sham-operated mouse kidney. Furthermore, in the case of the I/R-operated mouse kidney, several larger molecular size bands (indicated by arrows), which probably correspond to DSP cross-linked complexes of S-MBP and meprin β, were observed. It should be noted that the protein bands of meprins and S-MBP, which were immunoprecipitated directly with the same amounts of the respective specific antibodies, were essentially the same either from the I/R-operated mouse kidneys or from the sham-operated mouse kidneys under the conditions examined (data not shown). Taken together, these results indicated that S-MBP and meprins were located close enough to interact with each other in the I/R-operated mouse kidney.

This interaction of S-MBP with meprins in the I/R-operated mouse kidney was further confirmed by in situ PLA of the kidney section. The requirement for dual recombination of pairs of antibodies in combination with very potent signal amplification makes in situ PLA, a powerful tool for identifying numerous interacting proteins and also their subcellular distributions (Söderberg et al. 2006). As shown in the diagram in Figure 3C, when S-MBP and meprins are within 40 nm in proximity, oligonucleotides (plus and minus chains) conjugated with secondary antibodies will hybridize each other to form a circular oligonucleotide. A DNA polymerase will generate a repeated sequence product extended from the circular oligonucleotide as a template. The repeated sequence product will be hybridized to Tex613 fluorophore-labeled oligonucleotide probes. The fluorescent signals indicate the proximity of S-MBP and meprins in situ. As shown in Figure 3D, Tex613 fluorescent signals, which indicate in situ proximity of S-MBP and meprin β, were observed on the base of the brush border of the proximal tubular epithelial cells of the I/R-operated mouse kidney, whereas essentially no signal was detected in the sham-operated mouse kidney. Similarly, essentially no signal was detected in the negative controls that had undergone staining without either primary antibody (neither anti-S-MBP nor anti-meprin β) or without either of the paired primary antibodies (either anti-S-MBP or anti-meprin β) (data not shown). In addition, a signal reflecting the proximity of S-MBP and meprin α was observed in the same manner as for meprin β (data not shown). These results indicate convincingly that S-MBP interacts with meprins in vivo to form macromolecular complexes, which may induce the activation of complement in the I/R-operated mouse kidney.

The activation of complement through the interaction of S-MBP with meprins in vitro

In order to determine whether the interaction of MBP with meprins activates complement, we developed an enzyme-linked immunosorbent assay (ELISA) system involving purified meprins from the normal mouse kidneys and recombinant mouse MBPs. In this assay system, microtiter wells were coated with biotinylated meprins or IgM Fc and filled with or without recombinant mouse S- or L-MBP. Subsequently, human C4 was added to the wells and then the deposited C4b was detected by adding horseradish peroxidase (HRP)-conjugated anti-human C4 monoclonal antibody (mAb). IgM Fc was used as a positive control, since IgM Fc is known to be a good ligand for MBP due to high-mannose-type *N*-glycans attached to the molecule. As shown in Figure 4, meprins demonstrated a remarkable